Geobios 51 (2018) 335–358

Available online at
ScienceDirect
www.sciencedirect.com

Elsevier Masson France
EM|consulte
www.em-consulte.com

Research paper

Late Quaternary to Recent diversity of fish otoliths from the Red Sea, central Mediterranean, and NE Atlantic sea bottoms☆

Chien-Hsiang Lin [a,b,*,1], Yun-Peng Chiang [c], Víctor Manuel Tuset [d], Antoni Lombarte [d], Angela Girone [b]

[a] Smithsonian Tropical Research Institute, PO Box 0843-03092, Balboa, Panama
[b] Dipartimento di Scienze della Terra e Geoambientali, Università degli Studi di Bari Aldo Moro, via E. Orabona, 4, 70125 Bari, Italy
[c] Institute of Ecology and Evolutionary Biology, College of Life Science, National Taiwan University, No. 1, Sec. 4, Roosevelt Rd., 10617 Taipei, Taiwan
[d] Institut de Ciències del Mar, Consejo Superior de Investigaciones Científicas, Passeig Marítim de la Barceloneta 37-49, 08003 Barcelona, Catalonia, Spain

ARTICLE INFO

Article history:
Received 2 February 2018
Accepted 25 June 2018
Available online 2 July 2018

Keywords:
Fish community
Taxonomy
Diversity estimator
Multivariate analysis
Paleoecology
Biogeography

ABSTRACT

Despite extensive studies on the taxonomy of fossil otoliths, the diversity of late Quaternary to Recent sea bottom otolith assemblages remains largely unexplored. Otolith assemblages from bottom sediments of the North-eastern Atlantic (NE Atlantic), central Mediterranean, and Red Sea were described based on a dataset of 9696 identifiable otoliths. Diversity estimators were computed and taxonomic compositions were compared against geographical site and depth gradient. Several species from the Red Sea show previously unnoticed range extensions or ancient occurrences, suggesting that the otolith assemblage requires further exploration in this region. The diversity is high in the NE Atlantic and central Mediterranean, whereas Red Sea assemblages are dominated by few taxa. We find that, departing from Modern fish communities, the richness of otolith taxa peaks at mid-water depths (500–1500 m) and decreases at depths > 2000 m. The lower diversity at shallow water suggests environments not favorable for otolith preservation. The assemblages are geographically distinct, due to unique combinations of mesopelagic taxa specific to each sample area, though areas in the central Mediterranean and middle-latitude NE Atlantic share many taxa. Depth does not seem to structure otolith assemblages in the central Mediterranean because the otolith composition in this region is highly variable at depths < 500 m but poorly variable at greater depths. The discrepancies between otolith thanatocoenoses and fossil assemblages and the potential application for reconstructing ancient fish communities are discussed. Illustrating otoliths that are rarely found in the literature, this study is the first descriptive and comparative diversity analysis on Recent otolith assemblages for the regions of interest.

1. Introduction

Fish otoliths are a significant biogenic component in superficial sea bottom sediments (Schwarzhans, 2013a; Lin, 2016; Lin et al., 2016, 2017b); their nearly ubiquitous nature in marine sediments is of particular interest to paleontological studies. Geologically young sea bottom otolith assemblages are likely to contain only the extant taxa (Lin et al., 2017b). A well-known Present environmental setting is therefore necessary to compare these assemblages with Modern fish communities. Such comparison provides a unique means for understanding the relation between recently dead (otolith thanatocoenoses) and living fish assemblages (fish biocoenoses) (e.g., Laptikhovsky et al., 2018), as well as an insight into evaluating how much information is lost in the fossilization process. Therefore, detailed studies on sea bottom otoliths are necessary for validating any paleoecological or paleobiogeographical reconstruction based on fossil otoliths. Nevertheless, related studies are so far very scarce (Schwarzhans, 2013a; Lin et al., 2016, 2017b).

Although geographically adjacent, the Modern semi-enclosed Mediterranean Sea and Red Sea represent two distinct teleost faunas (Ormond and Edwards, 1987; Bianchi et al., 2012). The Red Sea contains many species distributed in the west Indo-Pacific realm (e.g., Righton et al., 1996; DiBattista et al., 2013), which are

☆ Corresponding editor: Gilles Escarguel.
* Corresponding author. Smithsonian Tropical Research Institute, PO Box 0843-03092, Balboa, Panama.
E-mail address: chlin.otolith@gmail.com (C.-H. Lin).
[1] Current address: Center for Tropical Ecology and Biodiversity, Tunghai University, Taiwan.

https://doi.org/10.1016/j.geobios.2018.06.002
0016-6995/

rarely found in the Mediterranean realm. Several studies, however, have indicated a number of Red Sea species invading the Mediterranean, and *vice versa* (e.g., Ben-Tuvia, 1964, 1966; Galil, 2000; Goren and Galil, 2005). On the other hand, the fish fauna in the Mediterranean share many species with fauna of the Northeastern Atlantic (NE Atlantic) (Almada et al., 2001; Domingues et al., 2005). Tracing back in the fossil record of otoliths, however, shows that the ancient Mediterranean fish fauna was very different from the Present one (Gaudant, 2002; Patarnello et al., 2007; Bianchi et al., 2012). It has been deeply transformed by regional geological events. In the early Miocene, the deep-water Mediterranean fish fauna shows similarity with the Present-day Atlantic-Mediterranean one, at least at the otolith-based genus level (Nolf and Brzobohatý, 2004; Lin et al., 2017a). The subsequent loss of a connection to the Indo-Pacific (the Red Sea) and several connections to the Paratethys and the Atlantic then shaped a distinct Miocene Mediterranean fish fauna (Emig and Geistdoerfer, 2004; Patarnello et al., 2007; Bianchi et al., 2012; Lin et al., 2015, 2017a). From the Plio-Pleistocene onwards, a shift towards the Modern Mediterranean fauna had finally become evident (Emig and Geistdoerfer, 2004; Girone et al., 2010; Bianchi et al., 2012; Lin et al., 2017a). However, it was not until the late Pliocene that the Mediterranean fish fauna became similar to NE Atlantic fauna, with many shared species and an almost complete absence of the Recent Indo-Pacific taxa (Emig and Geistdoerfer, 2004; Patarnello et al., 2007; Nolf and Girone, 2006).

The species composition of seafloor otolith assemblages is expected to reflect the regional fish fauna, thus samples from the Mediterranean will likely reflect the Mediterranean fish community and share much more taxa with the NE Atlantic samples than the Red Sea ones. In addition, as in studies based on extant faunas, diversity estimators of otolith samples could be correlated to depth and/or geographical location. To test this assumption, we first achieve a detailed taxonomic assignment of otoliths from the NE Atlantic, the central Mediterranean and the Red Sea bottoms, the last one still being poorly known with respect to otolith assemblages. Then, we quantify the local diversity and make comparisons among samples at different depths and locations using various multivariate statistical analyses.

2. Material and methods

2.1. Sediment sampling

Sediment samples are summarized in Table 1, and Fig. 1 depicts the study areas (detailed coordinates and depth of each sample station are given in Appendices A–C). As in Lin et al. (2016), 41 samples were collected from the NE Atlantic; otoliths were prepared by André Freiwald (Wilhelmshaven). The Van Veen grab and box corer were employed during the ALKOR 232 cruise in the North Sea (NS), the M61/1 and GeoB8045-1 cruises in the high-latitude NE Atlantic (HNEA), and the M60/1, VH-97 and GeoB9002-1 cruises in the middle-latitude NE Atlantic (MNEA).

Table 1
Summary of sea bottom samples.

Investigated area	Nb. of stations (samples)	Depth range (m)	Main coordinates
The North Sea	12	64–110	59°N; 10°E
High-latitude NEA	17	646–1059	51°N; 11°W and 56°N; 17W
Middle-latitude NEA	12	130–900	33°N; 14°W and 35°N; 12°W
Central Mediterranean	49	51–3300	39°-40°N; 12°-19°E
The Red Sea	11	393–2120	15°-27°N; 34°-41°E

A total of 49 sediment samples from the central Mediterranean (CM) were analyzed (samples originally deposited at the Instituto di Scienze Marine-Consiglio Nazionale delle Ricerche [ISMAR-CNR], Bologna, Italy). Sediments were collected during the RV Bannock cruises CJ72, T72, T73, T74, J73, and J74 by employing dredge devices (Sartori, 1977), and during the COCOMAP14 cruise by using grab devices (Lin et al., 2017b). Sediment samples were wet-sieved over a 500 μm mesh for extracting the otoliths.

The Red Sea (RS) otolith material was provided by Kristiaan Hoedemakers (Institut royal des Sciences naturelles de Belgique [IRSNB], Brussels, Belgium), and was originally prepared by Arie Janssen (Naturalis Biodiversity Center, Leiden, the Netherlands) during his investigation of the holoplanktonic mollusks (Janssen, 2007). A total of 11 samples have been included in the present study: six of them were collected during the Meteor 31/2 cruise, four during the Meteor Cruise 5, and a last sample comes from the Valdivia 29 cruise (Janssen, 2007: table 1). These sediment samples were mostly collected by box corer, ranging in depth from 393 to 2120 m b.s.l., and geographically spreading over almost the entire length of the Red Sea.

An extensive ecological analysis of this material is not performed here, due to uncertainties in the preparation procedure (e.g., sieving mesh size and total sediment quantity in a single sample) and lower total quantity of the material. However, a brief summary of taxa occurring in these sediment samples is presented. Each taxon is recorded with its depth range to evidence geographical distribution *vs.* bathymetry. The taxa were further divided into pelagic and benthic-benthopelagic groups (Girone, 2003, 2005, 2007) and quantitatively analyzed separately in order to evaluate the dominance of any given taxon (see Lin et al., 2016 for details). Identifiable otoliths were assigned to the lowest possible taxonomic level, and then used for quantitative analyses, excluding unidentified specimens such as juvenile otoliths without conclusive identification and poorly preserved specimens (juv. and indet. in Appendices A–C, respectively).

2.2. Diversity measures

Simpson's diversity index (D) and Pielou's evenness index (J') were computed by using the EstimateS software (Colwell, 2013) for different regions and at different depth intervals to evidence variations in diversity metrics. Sample-based rarefaction and extrapolation with 95% confidence intervals were also calculated using the EstimateS software for evaluating collection power and sample-size controlled richness (Gotelli and Colwell, 2011; Colwell, 2013).

2.3. Compositional analysis

Otolith abundance and composition in each station were quantitatively analyzed to evaluate the similarities and differences among sample assemblages. A Bray-Curtis dissimilarity matrix among assemblages was first calculated based on the square-root transformed abundances of each fish taxon within each assemblage. Then, a hierarchical cluster analysis using Ward's algorithm (Legendre and Anderson, 1999; Nicolas et al., 2010) and a principal coordinate analysis (PCoA) with centroid distances were performed on the Bray-Curtis matrix in order to describe and compare the compositional discontinuities and continuities among the studied samples. These analyses were carried out using the functions *betadisper* and *permutest* from the *vegan* package (Oksanen et al., 2013) for the R software (R Core Team, 2012). Samples containing less than five otoliths were excluded.

Non-parametric one-way analysis of similarity (ANOSIM; Clarke, 1993) using the Bray-Curtis dissimilarity index was

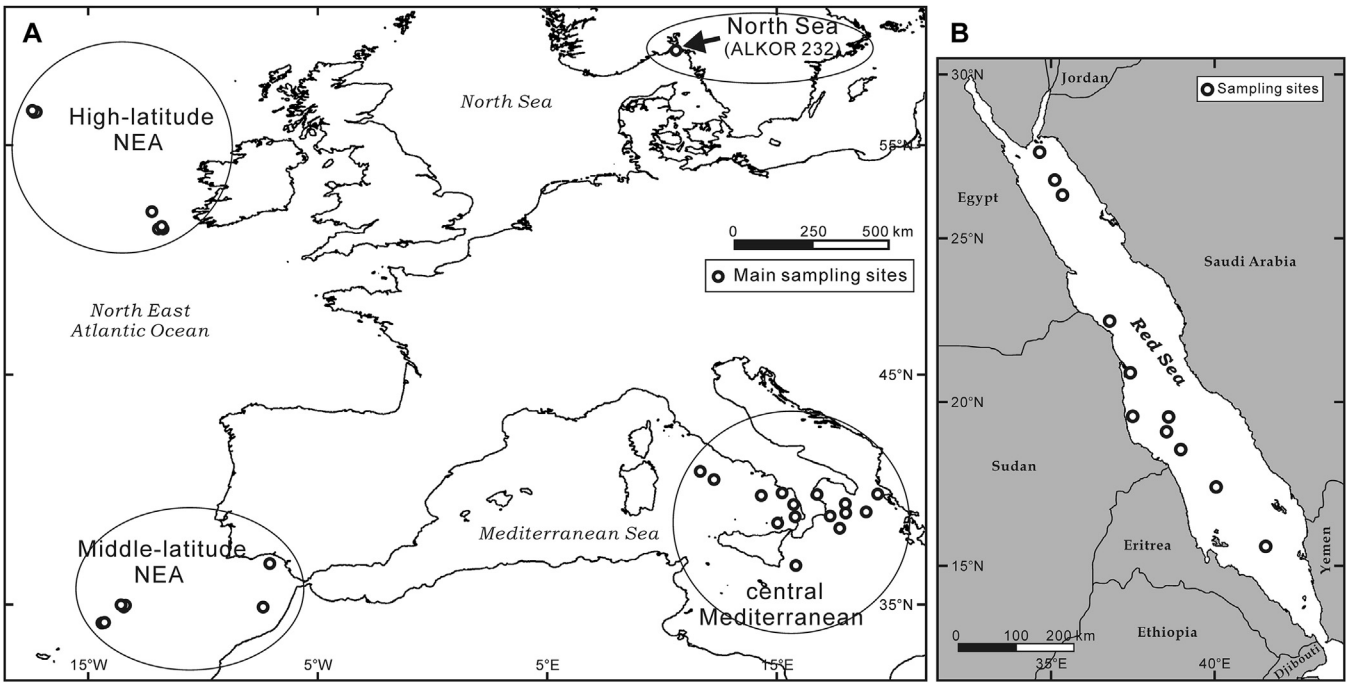

Fig. 1. Map showing the main sampling sites in the NE Atlantic and central Mediterranean (**A**) and in the Red Sea (**B**). See Appendices A–C for the coordinates and depth of each sample. Map derived from the EMODnet Bathymetry portal (http://www.emodnet-bathymetry.eu) and Janssen (2007).

achieved to statistically detect assemblage differences between the regions of interest. Samples were first depth-pooled in order to increase sample size (Lin et al., 2016). Two main intervals (< 500 m and 500–1000 m) were analyzed, deeper intervals being insufficient sampled. Since CM samples cover a complete depth range, a depth-structured one-way ANOSIM was also conducted to test compositional heterogeneities along the depth gradient in this region. The ANOSIM compares the average rank of similarities within the predefined groups of samples to the average rank of similarities between groups. Values of R close to 1 indicate strong between-group differences, while values close to 0 indicate a lack of differences between the predefined groups (Pusch et al., 2004). When a significant difference ($p < 0.05$) was detected, a similarity percentage analysis (SIMPER; Clarke, 1993) was conducted to determine which species were representatives of specific assemblages and their contribution to observed dissimilarities between each pair of groups (Pusch et al., 2004; Layman and Winemiller, 2005; García-Mederos et al., 2015). ANOSIM and SIMPER analyses were performed using the PAST software, v. 1.81 (Hammer et al., 2001).

3. Systematic paleontology

We obtained a total of 17,587 otoliths from the sediment samples, reducing to 9,696 identified otoliths after removing unidentifiable specimens. The otoliths identified were assigned to 141 taxa in 51 families (Table 2; Figs. 2–11). In addition to the list of otolith taxa recognized in this study, Table 2 also provides their abundance and depth range distribution. The classification follows Nelson et al. (2016). Only those taxa requiring further comments are listed below. Since the NE Atlantic and CM assemblages share many species, otolith figures (Figs. 2–9) and taxonomic remarks are presented together. All figured specimens are deposited in the otolith collections of the "Dipartimento di Scienze della Terra e Geoambientali, Università degli Studi di Bari Aldo Moro".

3.1. The NE Atlantic and central Mediterranean taxa

Class Osteichthyes Huxley, 1880
Order Anguilliformes Regan, 1909
Suborder Congroidei Nelson, 1984
Family Congridae Kaup, 1856
Genus ***Gnathophis*** Kaup, 1859
Gnathophis mystax (Delaroche, 1809)
Fig. 2(J–S)

Remarks: The otoliths of *G. mystax* are characterized by a thick and elliptic shape. The ventral rim bears a conspicuous angle slightly anterior to the middle part of the otolith. They possess a deep, obliquely inclined sulcus that runs downwards to the posterior side, and an ostium open widely to the anterodorsal rim. In some large specimens, there is a depression in the posterior part of the otolith. In CM samples, *G. mystax* otoliths of various sizes were recovered (Fig. 2(O–S)); this growth series clearly indicates that the morphology of the sulcus is consistent in all sizes, but the otolith outline changes from a nearly rectangular to a more elliptic shape and features such as a conspicuous angle on the ventral rim only start to appear at a later growth stage.

Order Alepocephaliformes Marshall, 1962
Family Alepocephalidae Bonaparte, 1846
Alepocephalidae indet.
Fig. 3(G–J)

Remarks: A single thick, high-bodied otolith from the high-latitude NE Atlantic (Fig. 3(G, H)) and a thinner one from the central Mediterranean (Fig. 3(I, J)) are recognized as members of alepocephalids. The NE Atlantic otolith possesses a deep incised, straight sulcus and an undulated, lobed ventral rim, suggesting the genus *Alepocephalus* (Smale et al., 1995: pl. 10, fig. E1); the central Mediterranean otolith is more similar to that of *Leptoderma macrops* Vaillant, 1886 (Nolf, 2013: pl. 42), which has a triangular outline and a sulcus without delimitated margins. However, precise allocations of these otoliths are not yet possible, due to insufficient alepocephalid otoliths for direct comparison. More-

Table 2
Otolith-based fish taxa identified in this study, with number of identified specimens and depth range from the sea bottoms of NE Atlantic, central Mediterranean, and Red Sea.

Fish otolith taxa from the sea bottoms of NE Atlantic, central Mediterranean and Red Sea	Illustration	NE Atlantic						Central Mediterranean		Red Sea	
		North Sea		High-latitude		Middle-latitude					
		Depth range (m)	Nb.	Depth range (m)	Nb.	Depth range (m)	Nb.	Depth range (m)	Nb.	Depth range (m)	Nb.
Nettastoma melanurum Rafinesque, 1810	Fig. 2(C–G)							1017–1060	5		
Conger conger (Linnaeus, 1758)	Fig. 2(A, B)					411	1	373	2		
Gnathophis mystax (Delaroche, 1809)	Fig. 2(J–S)					130–411	14	51–487	12		
Congridae indet.	Fig. 10(A)									393	1
Engraulis encrasicolus (Linnaeus, 1758)	Fig. 2(T–W)							51–1060	7		
Sardina pilchardus (Walbaum, 1792)	Fig. 2(H)							61–435	2		
Clupeidae indet.	Fig. 10(B, C)									1040	1
Maulisia mauli Parr, 1960	Fig. 2(F'–H')			854–912	4						
Xenodermichthys copei (Gill, 1884)	Fig. 2(I'–K')			646–912	5						
Alepocephalidae indet. 1	Fig. 3(G, H)			981	1						
Alepocephalidae indet. 2	Fig. 3(I, J)							1017–1060	1		
Glossanodon leioglossus (Valenciennes, 1848)	Fig. 2(I)					204	2	527	1		
Opisthoproctus grimaldii Zugmayer, 1911	Fig. 2(X, Y)					751	1				
Opisthoproctus soleatus Vaillant, 1888	Fig. 2(Z–B')			682	2	900	29				
Rhynchohyalus natalensis (G. et von Bonde, 1924)	Fig. 2(C')			863	1						
Nansenia groenlandica (Reinhardt, 1840)	Fig. 2(D' E')			881	1						
Bathylagus euryops Goode et Bean, 1896	Fig. 3(A–C)			813–981	62						
Gonostoma denudatum Rafinesque, 1810	Fig. 3(M)							1017–1060	1		
Margrethia obtusirostra Jespersen et Tåning, 1919	Fig. 3(D–F)					164–204	3				
Gonostomatidae indet.	Fig. 3(L)							1017–3300	18		
Maurolicus muelleri (Gmelin, 1789)	Fig. 3(Q, R)			1059	1	204–222	2	51–3300	1151		
Maurolicus sp.	Fig. 10(D, E)									393–2120	34
Valenciennellus tripunctulatus (Esmark, 1871)	Fig. 3(X)					751	1				
Argyropelecus hemigymnus Cocco, 1829	Fig. 3(K)							433–1060	7		
Ichthyococcus ovatus (Cocco, 1838)	Fig. 3(O, P)					411	1	380–3300	105		
Ichthyococcus sp.	Fig. 10(F)									772–779	1
Vinciguerria aff. *attenuata* (Cocco, 1838)	Fig. 3(N)							433–1227	5		
Vinciguerria poweriae (Cocco, 1838)	Fig. 3(S–W)					149–222	2	67–3300	256		
Chauliodus sloani Bloch et Schneider, 1801	Fig. 3(Y)							1017–1060	2		
Chlorophthalmus agassizi Bonaparte, 1840	Fig. 3(Z–B')							487–433	24		
Scopelarchus analis (Brauer, 1902)	Fig. 3(H')					130–800	51				
Evermannella balbo (Risso, 1820)	Fig. 4(A–D)							373–3300	25		
Sudis hyalina (Rafinesque, 1810)	Fig. 4(G, H)							3190–3300	1		
Arctozenus risso (Bonaparte, 1840)	Fig. 3(C'–G')							433–3300	105		
Paralepis coregonoides (Risso, 1820)	Fig. 3(I'–K')							433–2878	29		
Lestidiops jayakari (Boulenger, 1889)	Fig. 4(E, F)							433–2878	12		
Lestrolepis sp.	Fig. 10(G–I)									431–2120	8
Benthosema glaciale (Reinhardt, 1837)	Fig. 4(I)							380–3300	193		
Benthosema pterotum (Alcock, 1890)	Fig. 10(T–V)									393–2120	261
Benthosema suborbitale (Gilbert, 1913)	Fig. 4(X–Z)					204–222	4				
Bolinichthys indicus (N. et N., 1969)	Fig. 4(J, K)					130–751	11				
Ceratoscopelus maderensis (Lowe, 1839)	Fig. 4(L–O)			646–1059	11	130–900	279	51–3300	1001		
Ceratoscopelus warmingii (Lütken, 1892)	Fig. 4(P–R)			763–1059	8	149–794	125				
Diaphus arabicus Nafpaktitis, 1978	Fig. 10(O, P)									772–779	7
Diaphus coeruleus (Klunzinger, 1871)	Fig. 10(J–L)									393–2120	3
Diaphus garmani Gilbert, 1906	Fig. 10(M, N)									772–779	9
Diaphus holti Tåning, 1918	Fig. 4(V, W)			646	1	204–900	6	51–3300	95		
Diaphus metopoclampus (Cocco, 1829)	Fig. 4(F'–H')							1017–3300	6		
Diaphus ostenfeldi Tåning, 1932	Fig. 11(D)									772–779	1
Diaphus rafinesquii (Cocco, 1838)	Fig. 4(S–U)					164–751	2	373–3300	14		
Electrona risso (Cocco, 1829)	Fig. 4(I'–L')			646–1059	21	130–900	178	67–3300	363		
Hygophum benoiti (Cocco, 1838)	Fig. 4(A'–E')			1059	5	149–800	220	51–3300	1536		
Hygophum hygomii (Lütken, 1892)	Fig. 4(P'–T')					149–800	114	51–3300	929		
Lampadena chavesi Collett, 1905	Fig. 5(A, B)					222–751	2				
Lampadena luminosa (Garman, 1899)	Fig. 11(J–L)									772–779	6
Lampadena pontifex Krefft, 1970	Fig. 5(C, D)					900	1				
Lampadena speculigera Goode et Bean, 1896	Fig. 4(M'–O')			646–981	9						
Lampanyctus crocodilus (Risso, 1810)	Fig. 5(J–N)			646–1059	53	204–900	29	433–3300	74		
Lampanyctus macdonaldi (Goode et Bean, 1896)	Fig. 5(E–I)			733–1059	63						
Lampanyctus photonotus Parr, 1928	Fig. 5(R)					180–751	4				
Lampanyctus pusillus (Johnson, 1890)	Fig. 5(O–Q)			646–1059	4	164–411	6	435–3300	110		
Lampanyctus sp.	Fig. 10(Q, R)									772–779	8
Lobianchia dofleini (Zugmayer, 1911)	Fig. 5(S–U)			763–778	3	164–800	62	66–3300	146		
Lobianchia gemellarii (Cocco, 1838)	Fig. 5(Z–B')			778–981	6	900	20	1017–3300	59		
Myctophum aurolaternatum Garman, 1899	Fig. 10(S)									772–779	1
Myctophum punctatum Rafinesque, 1810	Fig. 5(C', D')			646–1059	11	149–900	27	51–3300	73		
Nannobrachium atrum (Tåning, 1928)	Fig. 5(V–Y)			763–913	4	222	2				
Nannobrachium sp.	Fig. 11(A–C)									772–779	2
Notoscopelus bolini Nafpaktitis, 1975	Fig. 5(J')							1017–3300	4		
Notoscopelus caudispinosus (Johnson, 1863)	Fig. 5(G')					222	1				
Notoscopelus elongatus (Costa, 1844)	Fig. 5(H', I')							373–3300	38		

Table 2 (*Continued*)

Fish otolith taxa from the sea bottoms of NE Atlantic, central Mediterranean and Red Sea	Illustration	NE Atlantic						Central Mediterranean		Red Sea	
		North Sea		High-latitude		Middle-latitude					
		Depth range (m)	Nb.	Depth range (m)	Nb.	Depth range (m)	Nb.	Depth range (m)	Nb.	Depth range (m)	Nb.
Notoscopelus kroyeri (Malm, 1861)	Fig. 5(E', F')			778–881	8						
Protomyctophum arcticum (Lütken, 1892)	Fig. 5(K'–M')			646–1059	34	800	3	494–3300	613		
Symbolophorus veranyi (Moreau, 1888)	Fig. 6(A–C)			646–1059	15	222–900	9	1017–3300	35		
Myctophidae indet.	Fig. 11(V, W)									685	1
Melanonus zugmayeri Norman, 1930	Fig. 7(O, P)			763–912	6	751	1				
Bathygadus melanobranchus Vaillant, 1888	Fig. 6(D, E)			682	1						
Coelorinchus caelorhincus (Risso, 1810)	Fig. 6(G–I)					800–900	4	487	4		
Coryphaenoides guentheri (Vaillant, 1888)	Fig. 6(J–M)			854–971	7						
Coryphaenoides mediterraneus (Giglioli, 1893)	Fig. 6(X, Y)			1059	1						
Hymenocephalus gracilis (Gilbert et Hubbs, 1920)	Fig. 6(N–P)					222–411	8				
Hymenocephalus italicus Giglioli, 1884	Fig. 6(S–U)							435–3300	9		
Nezumia aequalis (Günther, 1878)	Fig. 6(V, W)							1017–1060	1		
Macrouridae indet.	Fig. 6(Z–B')			682–912	2						
Trachyrincus scabrus (Rafinesque, 1810)	Fig. 6(F)					900	1				
Gadella maraldi (Risso, 1810)	Fig. 6(Q, R)							494–3300	4		
Laemonema sp.	Fig. 6(C', D')			682	1						
Lepidion sp.	Fig. 7(A–E)			863	1	900	3				
Mora moro (Risso, 1810)	Fig. 7(K, L)			646–778	7			1017–1060	3		
Physiculus dalwigki Kaup, 1858	Fig. 7(I, J)					900	1				
Merluccius merluccius (Linnaeus, 1758)	Fig. 7(Q)	64–88	5	646–1059	15			435–1227	28		
Raniceps raninus (Linnaeus, 1758)	Fig. 7(Z, A')	64–102	2								
Bregmaceros sp.	Fig. 11(E, F)									393–2120	20
Phycis blennoides (Brünnich, 1768)	Fig. 6(E', F')					900	1	67–1060	10		
Gaidropsarus sp.	Fig. 7(R)							433	1		
Ciliata mustela (Linnaeus, 1758)	Fig. 7(X, Y)	64	1								
Gadiculus argenteus Guichenot, 1850	Fig. 7(M, N)			646–981	10	900	1	373–3300	35		
Micromesistius poutassou (Risso, 1827)	Fig. 7(F–H)	64–75	8	646–1059	45	900	14	51–1227	12		
Pollachius pollachius (Linnaeus, 1758)	Fig. 7(S, T)	102	1								
Trisopterus esmarkii (Nilsson, 1855)	Fig. 7(U–W)	64–102	40								
Trisopterus luscus (Linnaeus, 1758)	Fig. 7(D'–F')	75–102	5			900	2				
Trisopterus minutus (Linnaeus, 1758)	Fig. 7(B')	64–102	14					487	1		
Myripristis sp.	Fig. 11(O–R)									685–2120	5
Diretmus argenteus Johnson, 1864	Fig. 8(I, J)			682–763	2	900	22				
Hoplostethus sp.	Fig. 11(X, Y)									1040	1
Melamphaes sp.	Fig. 8(R, S)			912–1059	2	130–800	7				
Poromitra megalops (Lütken, 1878)	Fig. 8(E–H)			854–981	20						
Scopelogadus beanii (Günther, 1887)	Fig. 8(K–N)			646–1059	151	800–900	2				
Carapus acus (Brünnich, 1768)	Fig. 7(C')							51–435	3		
Echiodon drummondii Thompson, 1837	Fig. 7(G', H')	64	1								
Bellottia apoda Giglioli, 1883	Fig. 7(I'–K')							380–487	6		
Bythitidae indet.	Fig. 8(A–D)			646–763	2	900	1				
Apogon sp.	Fig. 8(A'–D')							51–1227	12		
Apogonidae indet.	Fig. 11(G–I)									393–2120	25
Deltentosteus quadrimaculatus (V., 1837)	Fig. 9(L)							373–435	5		
Gobius niger Linnaeus, 1758	Fig. 9(O, P)							51–487	19		
Gobius paganellus Linnaeus, 1758	Fig. 9(N)							66	4		
Lesueurigobius friesii (Malm, 1874)	Fig. 9(U)	64	1					373–380	7		
Lesueurigobius suerii (Risso, 1810)	Fig. 9(V)							61–95	3		
Pomatoschistus sp.	Fig. 9(M)	64	1								
Blennius ocellaris Linnaeus, 1758	Fig. 9(J, K)							51	1		
Hemiramphidae indet.	Fig. 11(M, N)									772–779	1
Trachurus picturatus (Bowdich, 1825)	Fig. 8(K', L')					186	1				
Carangidae indet.	Fig. 8(E', F')							904–950	1		
Arnoglossus sp.	Fig. 9(A'–C')							435–487	5		
Bathysolea profundicola (Vaillant, 1888)	Fig. 9(S, T)							1017–1060	1		
Callionymus maculatus Rafinesque, 1810	Fig. 9(H, I)							373	1		
Trichiurus sp.	Fig. 11(S–U)									393–685	5
Trichiuridae indet.	Fig. 9(D')							433–435	2		
Cubiceps gracilis (Lowe, 1843)	Fig. 9(W–Z)					130–800	40	3190–3300	5		
Cubiceps sp.	Fig. 11(Z)									685–779	4
Epigonus constanciae (Giglioli, 1880)	Fig. 8(O–Q)					411	3	373–3300	12		
Epigonus denticulatus Dieuzeide, 1950	Fig. 8(Z)							3190–3300	2		
Mullidae indet.	Fig. 9(D–F)							433–1060	2		
Anthias anthias (Linnaeus, 1758)	Fig. 8(I', J')							79	1		
Cepola macrophthalma (Linnaeus, 1758)	Fig. 9(G)							51–487	8		
Helicolenus dactylopterus (Delaroche, 1809)	Fig. 8(W–Y)							373–433	2		
Scorpaenidae indet.	Fig. 8(T–V)					411	1	51–91	2		
Pagellus acarne (Risso, 1827)	Fig. 9(A–C)							51–487	2		
Spicara sp.	Fig. 8(G', H')					186–411	6				
Capros aper (Linnaeus, 1758)	Fig. 9(Q, R)					164	1				
Total number of identified otoliths			**79**		**606**		**1332**		**7274**		**405**

Classification following Nelson et al. (2016).

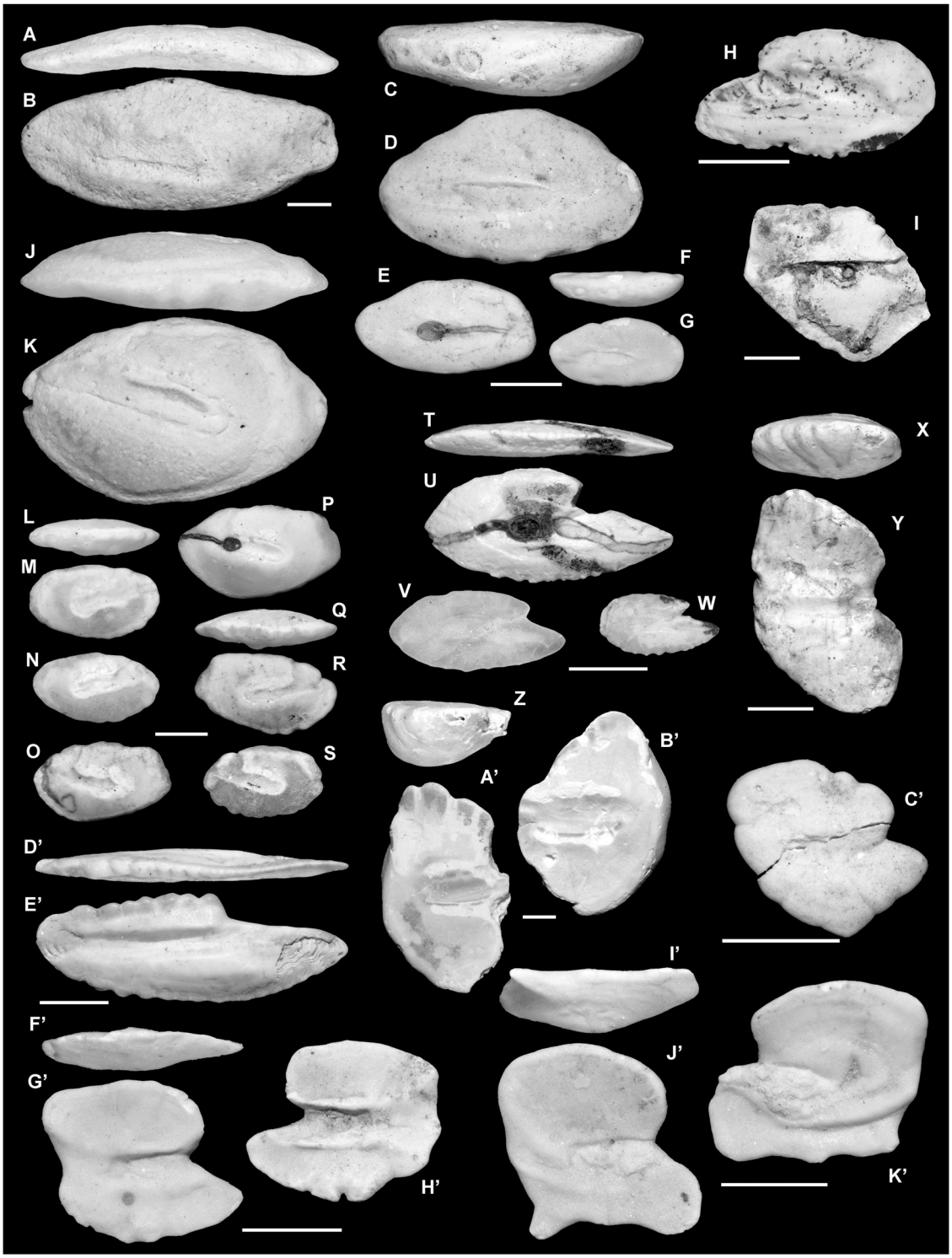

Fig. 2. Fish otoliths from the high- and middle-latitude North-eastern Atlantic (HNEA and MNEA) and central Mediterranean (CM) sea bottoms. Pictures are inner views unless otherwise indicated. **A, B.** *Conger conger*, MNEA, M60/1-309 (411 m); A: ventral view. **C–G.** *Nettastoma melanurum*, CM, J74-12 (1017–1060 m); C, F: ventral views. **H.** *Sardina pilchardus*, CM, COCOMAP14-33 (435 m). **I.** *Glossanodon leioglossus*, CM, COCOMAP14-26 (527 m). **J–S.** *Gnathophis mystax*; J–N: MNEA: J, K, M60/1-765 (222 m); L–N, VH97-103 (164 m); O–S: CM: O, Q, R, COCOMAP14-31 (373 m); P, COCOMAP14-34 (487 m); S, T73-12 (61 m) ; J, L, Q, ventral views. **T–W**. *Engraulis encrasicolus*, CM, T–V, COCOMAP14-32 (380 m); W: J74-12 (1017–1060 m); T: ventral view. **X, Y**. *Opisthoproctus grimaldii*, MNEA, VH97-104 (751 m); X: ventral view. **Z–B'**. *Opisthoproctus soleatus*, MNEA, GeoB9002-1 (*ca.* 900 m); Z: ventral view. **C'**. *Rhynchohyalus natalensis*, HNEA, M61/1-300 (863 m). **D', E'**. *Nansenia groenlandica*, HNEA, M61/1-242 (881 m); D': ventral view. **F'–H'**. *Maulisia mauli*, HNEA, M61/1-225 (912 m); F': ventral view. **I'–K'**. *Xenodermichthys copei*, HNEA, M61/1-225 (912 m); I': ventral view. Scale bars: 1 mm.

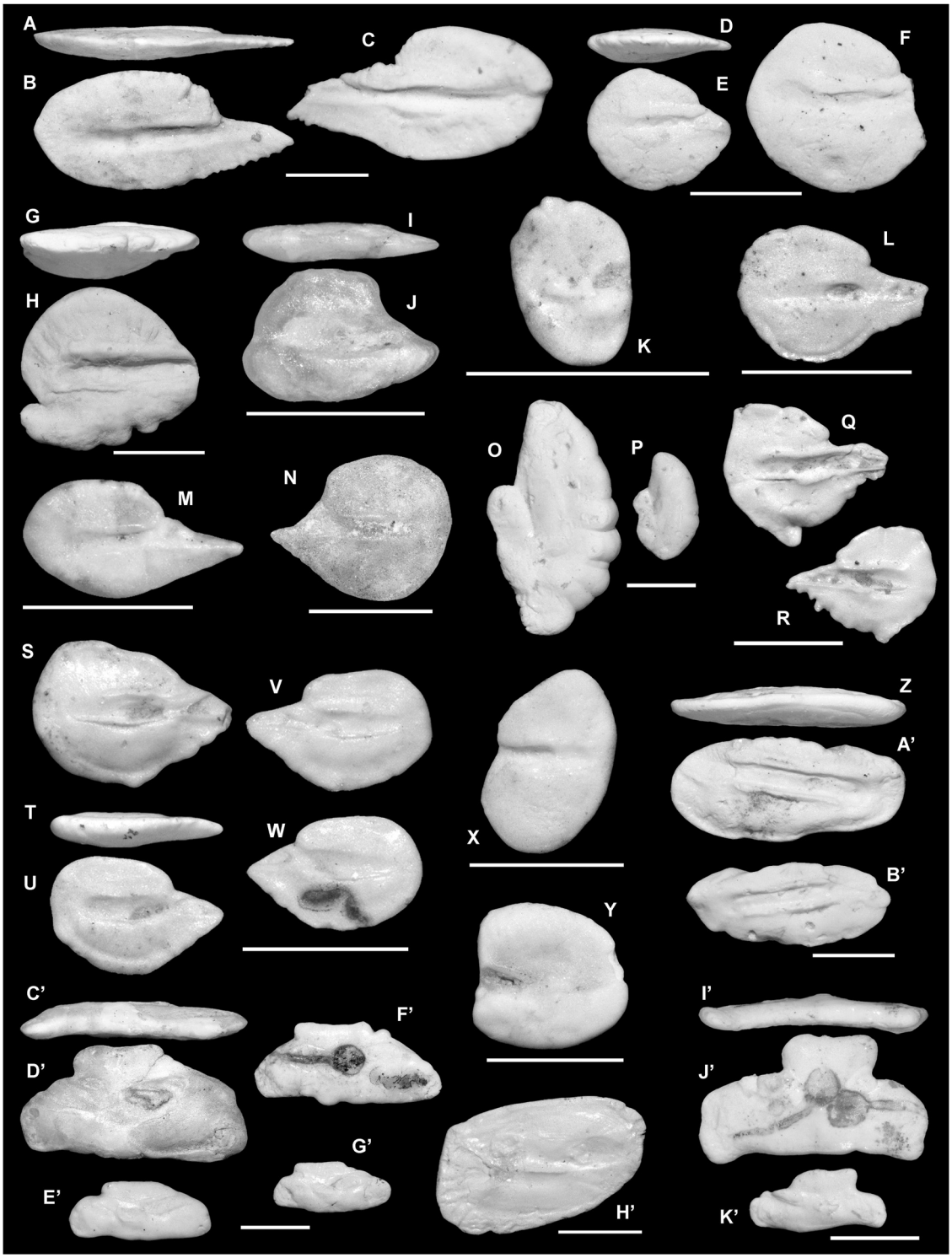

Fig. 3. Fish otoliths from the high- and middle-latitude North-eastern Atlantic (HNEA and MNEA) and central Mediterranean (CM) sea bottoms. Pictures are inner views unless otherwise indicated. **A–C.** *Bathylagus euryops*, HNEA, M61/1-225 (912 m); A: ventral view. **D–F.** *Margrethia obtusirostra*, MNEA; D, E: VH97-103 (164 m); F: VH97-94 (204 m); D: ventral view. **G, H.** Alepocephalidae indet. 1, HNEA, M61/1-224 (981 m); G: ventral view. **I, J.** Alepocephalidae indet. 2, CM, J74-12 (1017–1060 m); I: ventral view. **K.** *Argyropelecus hemigymnus*, CM, COCOMAP14-24 (433 m). **L.** Gonostomatidae indet., CM, J74-12 (1017–1060 m). **M.** *Gonostoma denudatum*, CM, J74-12 (1017–1060 m). **N.** *Vinciguerria* aff. *attenuata*, CM, J74-20 (1227 m). **O, P.** *Ichthyococcus ovatus*, CM, T72-41 (3190–3300 m). **Q, R.** *Maurolicus* m*uelleri*, CM, J74-12 (1017–1060 m). **S–W.** *Vinciguerria poweriae*, CM, J74-12 (1017–1060 m); T: ventral view. **X.** *Valenciennellus tripunctulatus*, MNEA, VH97-104 (751 m). **Y.** *Chauliodus sloani*, CM, J74-12 (1017–1060 m). **Z–B'.** *Chlorophthalmus agassizi*, CM, COCOMAP14-33 (435 m); Z: ventral view. **C'–G'.** *Arctozenus risso*, CM; C'–E': J74-20 (1227 m); F', G': COCOMAP14-24 (433 m); C': ventral view. **H'.** *Scopelarchus analis*, MNEA, VH97-94 (204 m). **I'–K'.** *Paralepis coregonoides*, CM, COCOMAP14-24 (433 m); I': ventral view. Scale bars: 1 mm.

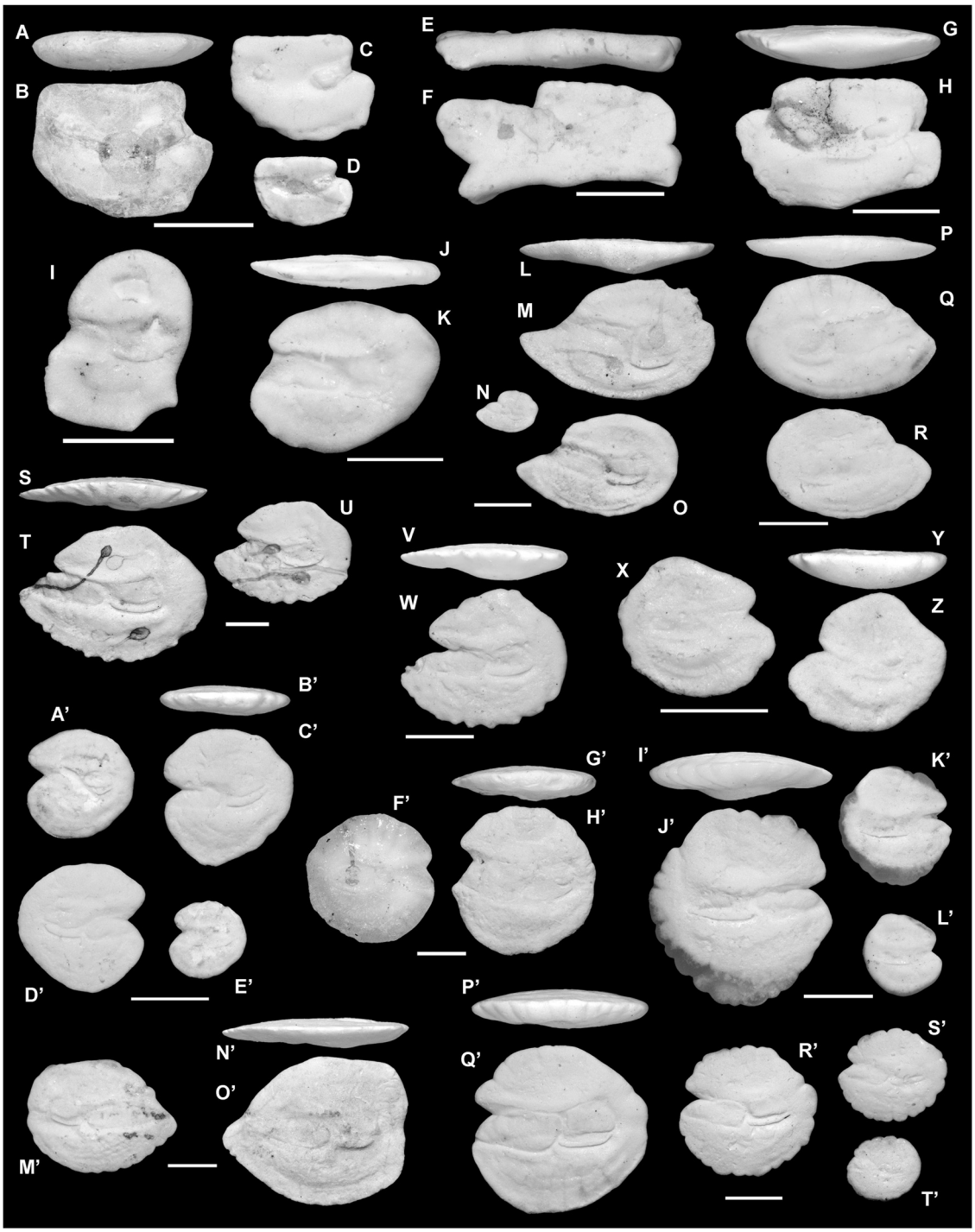

Fig. 4. Fish otoliths from the high- and middle-latitude North-eastern Atlantic (HNEA and MNEA) and central Mediterranean (CM) sea bottoms. Pictures are inner views unless otherwise indicated. **A–D.** *Evermannella balbo*, CM; A, B: COCOMAP14-24 (433 m); C, D: J74-20 (1227 m); A: ventral view. **E, F.** *Lestidiops jayakari*, CM, COCOMAP14-24 (433 m); E: ventral view. **G, H.** *Sudis hyalina*, CM, T72-41 (3190–3300 m); G: ventral view. **I.** *Benthosema glaciale*, CM, T72-41 (3190–3300 m). **J, K.** *Bolinichthys indicus*, MNEA, VH97-94 (204 m); J: ventral view. **L-O.** *Ceratoscopelus maderensis*, CM, T72-41 (3190–3300 m); L: ventral view. **P–R.** *Ceratoscopelus warmingii*, MNEA, VH97-102 (149 m); P: ventral view. **S–U.** *Diaphus rafinesquii*, CM, T72-41 (3190-3300 m); S: ventral view. **V, W.** *Diaphus holti*, MNEA, M60/1-765 (222 m); V: ventral view. **X–Z.** *Benthosema suborbitale*, MNEA, M60/1-765 (222 m); Y: ventral view. **A'–E'.** *Hygophum benoiti*; A', E': HNEA, M61/1-221 (1059 m); B'–D': MNEA, M60/1-765 (222 m); B': ventral view. **F'–H'.** *Diaphus metopoclampus*, CM, J73-5 (2000–2042 m); G': ventral view. **I'–L'.** *Electrona risso*, CM, J74-12 (1017–1060 m); I': ventral view. **M'–O'.** *Lampadena speculigera*, HNEA; M': M61/1-225 (912 m); N', O': M61/1-224 (981 m); N': ventral view. **P'–T'.** *Hygophum hygomii*, MNEA, M60/1-765 (222 m); P': ventral view. Scale bars: 1 mm.

over, alepocephalid otoliths commonly show a great intraspecific variability (Smale et al., 1995; Nolf and Brzobohatý, 1994: pl. 2, figs. 1–4) which impedes confident identification.

Order Stomiiformes Regan, 1909
Suborder Phosichthyoidei Weitzman, 1974
Family Phosichthyidae Weitzman, 1974
Genus ***Vinciguerria*** Jordan et Evermann, 1896
Vinciguerria aff. *attenuata* (Cocco, 1838)
Fig. 3(N)

Remarks: The outline of these otoliths shows a superficial resemblance to that of *Bonapartia pedaliota* Goode et Bean, 1896, a

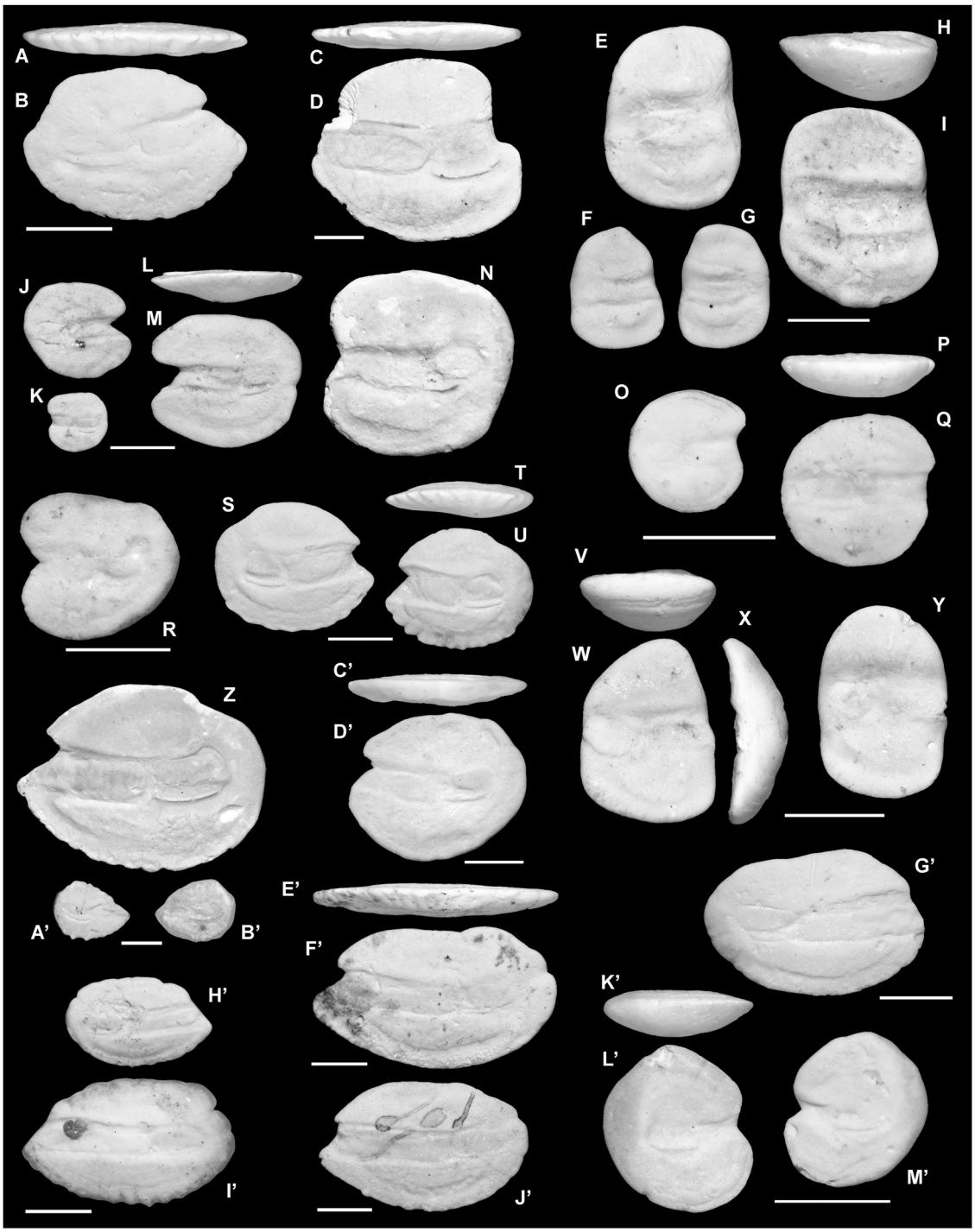

Fig. 5. Fish otoliths from the high- and middle-latitude North-eastern Atlantic (HNEA and MNEA) and central Mediterranean (CM) sea bottoms. Pictures are inner views unless otherwise indicated. **A, B.** *Lampadena chavesi*, MNEA, M60/1-765 (222 m); A: ventral view. **C, D.** *Lampadena pontifex*, MNEA, GeoB9002-1 (*ca*. 900 m); C: ventral view. **E–I.** *Lampanyctus* m*acdonaldi*, HNEA; E, H, I: M61/1-221 (1059 m); F, G: M61/1-304 (913 m); H: ventral view. **J–N.** *Lampanyctus crocodilus*; J–M: CM, J74-12 (1017–1060 m); N: MNEA, GeoB9002-1 (*ca*. 900 m); L: ventral view. **O–Q.** *Lampanyctus pusillus*, MNEA, M60/1-309 (411 m); P: ventral view. **R.** *Lampanyctus photonotus*, MNEA, M60/1-760 (180 m). **S–U.** *Lobianchia dofleini*, MNEA, M60/1-765 (222 m); T: ventral view. **V-Y.** *Nannobrachium atrum*, HNEA, M61/1-304 (913 m); V: ventral view; X: anterior view. **Z–B'.** *Lobianchia gemellarii*; Z: MNEA, GeoB9002-1 (*ca*. 900 m); A', B': CM, J74-12 (1017–1060 m). **C', D'.** *Myctophum punctatum*, MNEA, M60/1-765 (222 m); C': ventral view. **E', F'.** *Notoscopelus kroyeri*, HNEA, M61/1-242 (881 m); E': ventral view. **G'.** *Notoscopelus caudispinosus*, MNEA, M60/1-765 (222 m). **H', I'.** *Notoscopelus elongatus*, CM, COCOMAP14-24 (433 m). **J'.** *Notoscopelus bolini*, CM, T72-41 (3190–3300 m). **K'–M'.** *Protomyctophum arcticum*, HNEA, M61/1-273 (763 m); K': ventral view. Scale bars: 1 mm.

subtropical to tropical Atlantic and Indian Ocean species. There is a marked oval deepening at the center of the sulcus of *B. pedaliota* (Smale et al., 1995: pl. 11, figs. A1, A2); however, this feature is not observed in the present specimens. Indeed, the latter sulcus configuration better suggests a *Vinciguerria* otolith. The extant specimens of *V. attenuata* illustrated by Nolf and Brzobohatý (2002: pl. 4, figs. 5–9) exhibit a slenderer shape than the high-bodied otoliths figured here.

Order Myctophiformes Regan, 1911
Family Myctophidae Gill, 1893
Figs. 4–6

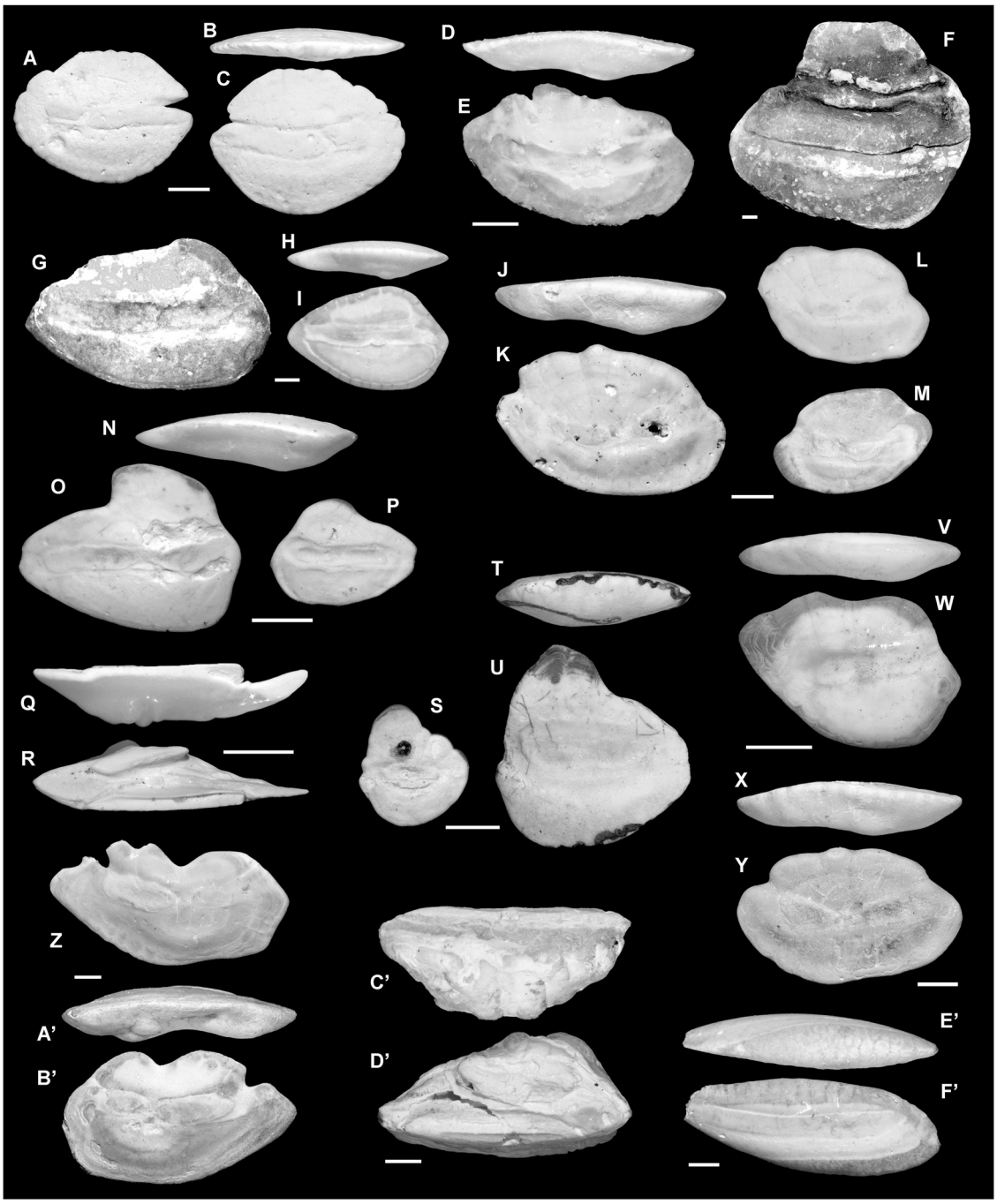

Fig. 6. Fish otoliths from the high- and middle-latitude North-eastern Atlantic (HNEA and MNEA) and central Mediterranean (CM) sea bottoms. Pictures are inner views unless otherwise indicated. **A–C.** *Symbolophorus veranyi*, MNEA, M60/1-765 (222 m); B: ventral view. **D, E.** *Bathygadus melanobranchus*, HNEA, GeoB8045-1 (682 m); D: ventral view. **F.** *Trachyrincus scabrus*, MNEA, GeoB9002-1 (*ca*. 900 m). **G–I.** *Coelorinchus caelorhincus*, MNEA, GeoB9002-1 (*ca*. 900 m); H: ventral view. **J–M.** *Coryphaenoides guentheri*, HNEA; J–L: M61/1-311 (971 m); M: M61/1-300 (863 m); J: ventral view. **N–P.** *Hymenocephalus gracilis*, MNEA, M60/1-309 (411 m); N: ventral view. **Q, R.** *Gadella maraldi* (Risso, 1810), CM, T72-41 (3190–3300 m); Q: ventral view. **S–U.** *Hymenocephalus italicus*, CM, COCOMAP14-34 (487 m); T: ventral view. **V, W.** *Nezumia aequalis*, CM, J74-12 (1017–1060 m); V: ventral view. **X, Y.** *Coryphaenoides mediterraneus*, HNEA, M61/1-221 (1059 m); X: ventral view. **Z–B'.** Macrouridae indet., HNEA; Z: M61/1-225 (912 m); A', B': GeoB8045-1 (682 m); A': ventral view. **C', D'.** *Laemonema* sp., HNEA, GeoB8045-1 (682 m); C': ventral view. **E', F'.** *Phycis blennoides*, MNEA, GeoB9002-1 (*ca*. 900 m); E': ventral view. Scale bars: 1 mm.

Remarks: Twenty-eight myctophid species were identified from the sea bottom samples, making helpful to comment here on some species that are not easily distinguished, although previous literature may also serve the same purpose (e.g., Brzobohatý and Nolf, 1996, 2000; Schwarzhans, 2013b). The otoliths of *Ceratoscopelus maderensis* (Lowe, 1839) are very similar to those of the congeneric *Ceratoscopelus warmingii* (Lütken, 1892) (Fig. 4(L–O) and Fig. 4(P–R), respectively); the former differ from the latter in having a highly protruding rostrum that is pointed at tip, forming a slightly upwardly bent anterior rim.

The otoliths of *Diaphus holti* Tåning, 1918 are characterized by a large dorsal area (Fig. 4(V, W)) which makes their overall shape higher than other *Diaphus* otoliths such as *Diaphus rafinesquii* (Cocco, 1838) (Fig. 4(S–U)). The rounded otoliths of *Diaphus*

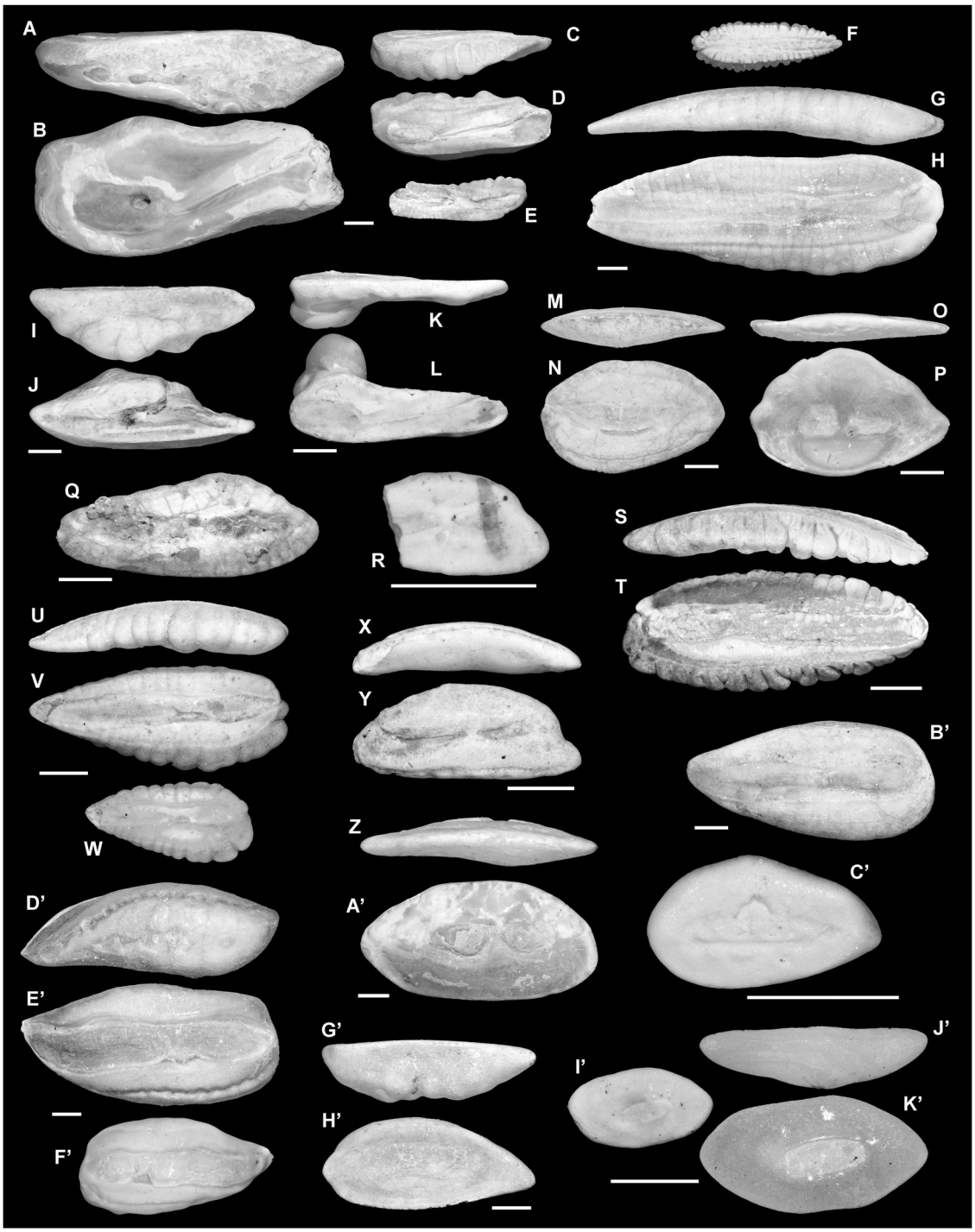

Fig. 7. Fish otoliths from the high- and middle-latitude North-eastern Atlantic (HNEA and MNEA), North Sea (NS), and central Mediterranean (CM) sea bottoms. Pictures are inner views unless otherwise indicated. **A–E.** *Lepidion* sp.; A, B: MNEA, GeoB9002-1 (*ca.* 900 m); C–E: HNEA, M61/1-300 (863 m); A, C: ventral views. **F–H.** *Micromesistius poutassou*; F: CM, J74-12 (1017–1060 m); G, H: NS, ALKOR 232-1144 (75 m); G: ventral view. **I, J.** *Physiculus dalwigki*, MNEA, GeoB9002-1 (*ca.* 900 m); I: ventral view. **K, L.** *Mora moro*, HNEA, M61/1-243 (778 m); K: ventral view. **M, N.** *Gadiculus argenteus*, HNEA, M61/1-225 (912 m); M: ventral view. **O, P.** *Melanonus zugmayeri*, HNEA, M61/1-225 (912 m); O: ventral view. **Q.** *Merluccius merluccius*, CM, COCOMAP14-34 (487 m). **R.** *Gaidropsarus* sp., CM, COCOMAP14-24 (433 m). **S, T.** *Pollachius pollachius*, NS, ALKOR 232-1146 (102 m); S: ventral view. **U–W.** *Trisopterus esmarkii*, NS, ALKOR 232-1147 (64 m); U: ventral view. **X, Y.** *Ciliata mustela*, NS, ALKOR 232-1147 (64 m); X: ventral view. **Z, A'.** *Raniceps raninus*, NS, ALKOR 232-1146 (102 m); Z: ventral view. **B'.** *Trisopterus minutus*, NS, ALKOR 232-1144 (75 m). **C'.** *Carapus acus*, CM, COCOMAP14-33 (435 m). **D'–F'.** *Trisopterus luscus*, NS; D', E': ALKOR 232-1144 (75 m); F'; ALKOR 232-1146 (102 m); D': ventral view. **G', H'.** *Echiodon drummondii*, NS, ALKOR 232-1147 (64 m); G': ventral view. **I'-K'.** *Bellottia apoda*, CM, COCOMAP14-32 (380 m); J': ventral view. Scale bars: 1 mm.

metopoclampus (Cocco, 1829) can be easily recognized (Fig. 4(F'–H')), and their posterior part is markedly more compact than that of *Hygophum hygomii* (Lütken, 1892) (Fig. 4(P'–T')), another species with oval to rounded otoliths.

The outline of *Electrona risso* (Cocco, 1829) and *Hygophum benoiti* (Cocco, 1838) otoliths show some similarities (Fig. 4(I'–L') and Fig. 4(A'–E'), respectively), but the larger dorsal area with a strong postero-dorsal angle can be observed only in the otoliths of

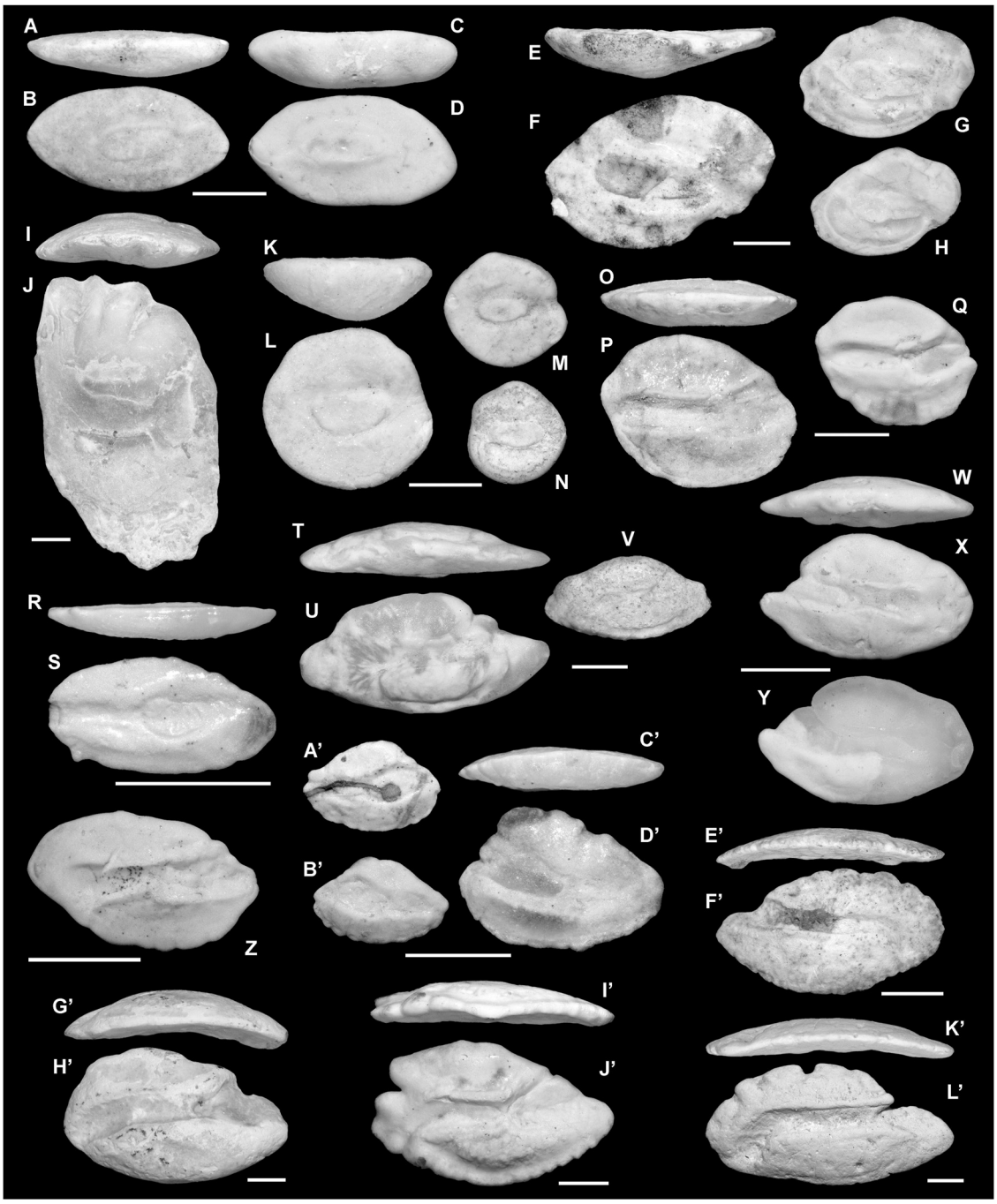

Fig. 8. Fish otoliths from the high- and middle-latitude North-eastern Atlantic (HNEA and MNEA) and central Mediterranean (CM) sea bottoms. Pictures are inner views unless otherwise indicated. **A–D.** Bythitidae indet.; A, B: MNEA, GeoB9002-1 (*ca.* 900 m); C, D: HNEA, M61/1-274; A, C: ventral views. **E–H.** *Poromitra megalops*, HNEA, M61/1-300 (863 m); E: ventral view. **I, J.** *Diretmus argenteus*, MNEA, GeoB9002-1 (*ca.* 900 m); I: ventral view. **K–N.** *Scopelogadus beanii*, HNEA, M61/1-221 (1059 m); K: ventral view. **O–Q.** *Epigonus constanciae* (Giglioli, 1880); O, P: MNEA, M60/1-309 (411 m); Q: CM, COCOMAP14-31 (373 m); O: ventral view. **R, S.** *Melamphaes* sp., MNEA, VH97-103 (164 m); R: ventral view. **T–V.** Scorpaenidae indet., CM; T, U: CJ72-7 (91 m); V: CJ72-14 (51 m); T: ventral view. **W–Y.** *Helicolenus dactylopterus*, CM; W, X: COCOMAP14-31 (373 m); Y: COCOMAP14-24 (433 m); W: ventral view. **Z.** *Epigonus denticulatus*, CM, T72-41 (3190–3300 m). **A'–D'.** *Apogon* sp., CM; A': J74-12 (1017–1060 m); B': J74-9 (1148 m); C', D': CJ72-14 (51 m); C': ventral view. **E', F'.** Carangidae indet., CM, CJ72-25 (904–950 m); E': ventral view. **G', H'.** *Spicara* sp., MNEA, M60/1-309 (411 m); G': ventral view. **I', J'.** *Anthias anthias*, CM, COCOMAP14-6 (79 m); I': ventral view. **K', L'.** *Trachurus picturatus*, MNEA, M60/1-758 (186 m); K': ventral view. Scale bars: 1 mm.

E. risso, while a more pointed ventral rim skewed in the anterior direction is observed only in *H. benoiti*. Moreover, the otoliths are thicker and the inner face is more convex in *E. risso*. The convexity of the inner face is also a key feature to distinguish juvenile specimens of *E. risso* from other myctophid otoliths (Fig. 4(L')).

Identification on the basis of juvenile and poorly preserved adult otoliths of *Notoscopelus* is highly speculative. An extensive otolith comparison within the genus has been provided in Brrzobohatý and Nolf (1996) and their basic criteria are followed here. The otoliths of *Notoscopelus caudispinosus* (Johnson, 1863) are the most distinct due to the highest otolith shape and a markedly elevated anterodorsal part (Fig. 5(G')). Recognition of the otoliths of other congeneric species is mainly based on the shape of their posterior rim: it is rather short and truncated in *Notoscopelus elongatus* (Costa, 1844) (Fig. 5(H', I')), and more extended in *N. bolini* Nafpaktitis, 1975 (Fig. 5(J')) and *N. kroyeri* (Malm, 1861)

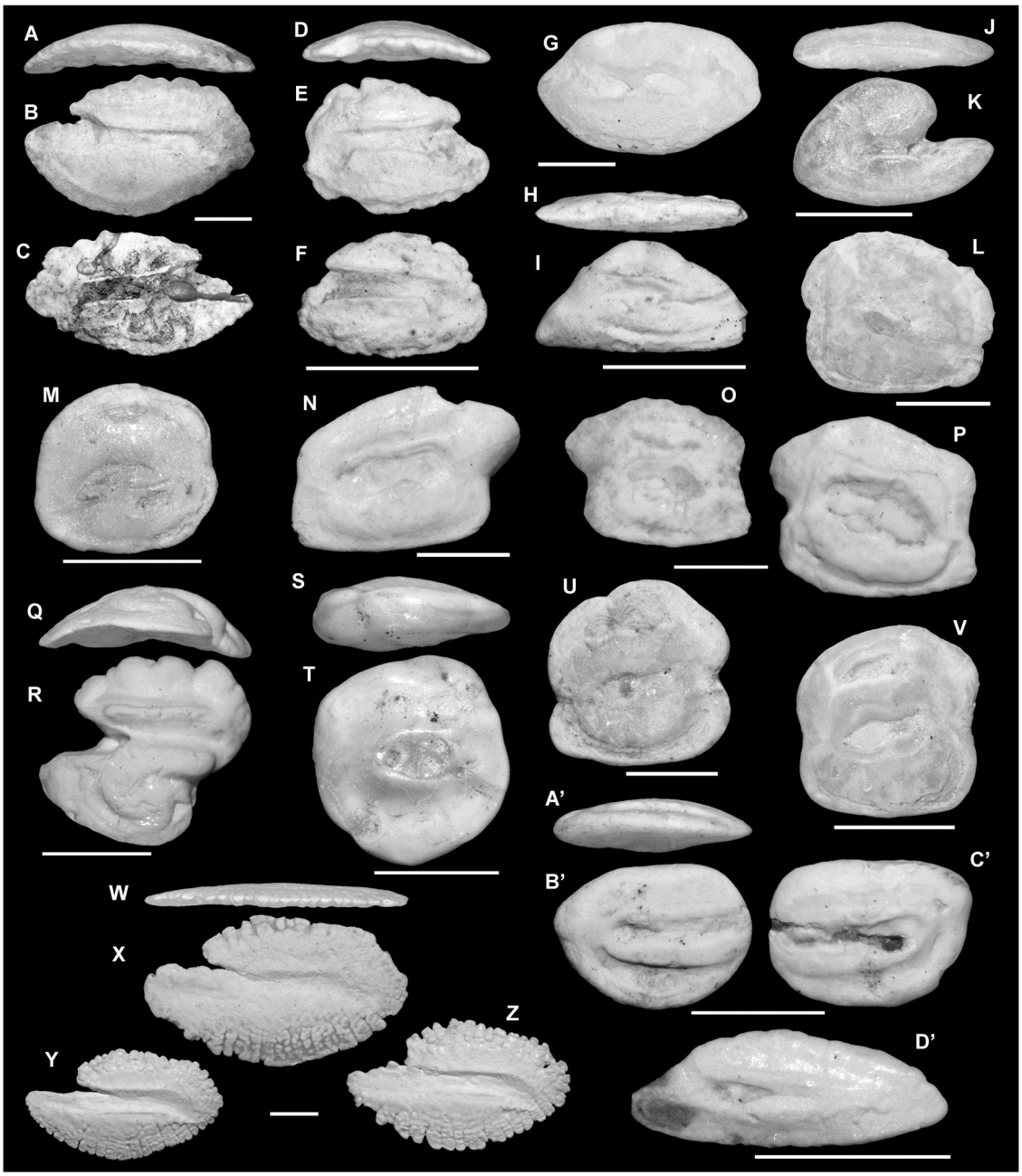

Fig. 9. Fish otoliths from the middle-latitude North-eastern Atlantic (MNEA), North Sea (NS), and central Mediterranean (CM) sea bottoms. Pictures are inner views unless otherwise indicated. **A–C.** *Pagellus acarne*, CM; A, B: CJ72-14 (51 m); C: COCOMAP14-34 (487 m); A: ventral view. **D–F.** Mullidae indet., CM; D, E: J74-12 (1017–1060 m); F: COCOMAP14-24 (433 m); D: ventral view. **G.** *Cepola macrophthalma*, CM, COCOMAP14-6 (79 m). **H, I.** *Callionymus maculatus*, CM, COCOMAP14-31 (373 m); H: ventral view. **J, K.** *Blennius ocellaris*, CM, CJ72-14 (51 m); J: ventral view. **L.** *Deltentosteus quadrimaculatus*, CM, COCOMAP14-32 (380 m). **M.** *Pomatoschistus* sp., NS, ALKOR 232-1147 (64 m). **N.** *Gobius paganellus*, CM, CJ72-6 (66 m). **O, P.** *Gobius niger*, CM, COCOMAP14-6 (79 m). **Q, R.** *Capros aper*, MNEA, VH97-103 (164 m); Q: ventral view. **S, T.** *Bathysolea profundicola*, CM, J74-12 (1017–1060 m); S: ventral view. **U.** *Lesueurigobius friesii*, NS, ALKOR 232-1147 (64 m). **V.** *Lesueurigobius suerii*, CM, T73-11 (95 m). **W–Z.** *Cubiceps gracilis*, MNEA; W, X: M60/1-758 (186 m); Y, Z: M60/1-765 (222 m); W: ventral view. **A'–C'.** *Arnoglossus* sp., CM, COCOMAP14-33 (435 m); A': ventral view. **D'.** Trichiuridae indet., CM, COCOMAP14-33 (435 m). Scale bars: 1 mm.

(Fig. 5(E', F')). In *N. bolini*, the postero-dorsal angle is followed by a deeper depression on the margin, while in *N. kroyeri*, the postero-dorsal angle is more rounded with an elevation on the margin.

The otoliths of *Protomyctophum arcticum* (Lütken, 1892) and *Benthosema glaciale* (Reinhardt, 1837) are both characterized by a high-bodied outline (Fig. 5(K'–M') and Fig. 4(I), respectively), but this is merely a superficial resemblance. The dorsal rim of *P. arcticum* is rather angular, making its highest point of the otolith in the middle, while in *B. glaciale* the dorsal rim is more rounded. Although it depends on the preservation status, the ventral rim of *B. glaciale* usually bears denticles, whereas all the rims are smooth in *P. arcticum*. Another difference, and perhaps more important for distinguishing poorly preserved specimens, is that the sulcus of *B. glaciale* is much deeper than that of *P. arcticum*, the latter being also less delimitated on both cristae.

Order Gadiformes Goodrich, 1909
Family Macrouridae Bonaparte, 1831
Macrouridae indet.
Fig. 6(Z–B')

Remarks: Two large macrourid otoliths were recovered from two high-latitude NE Atlantic samples. They very likely belong to

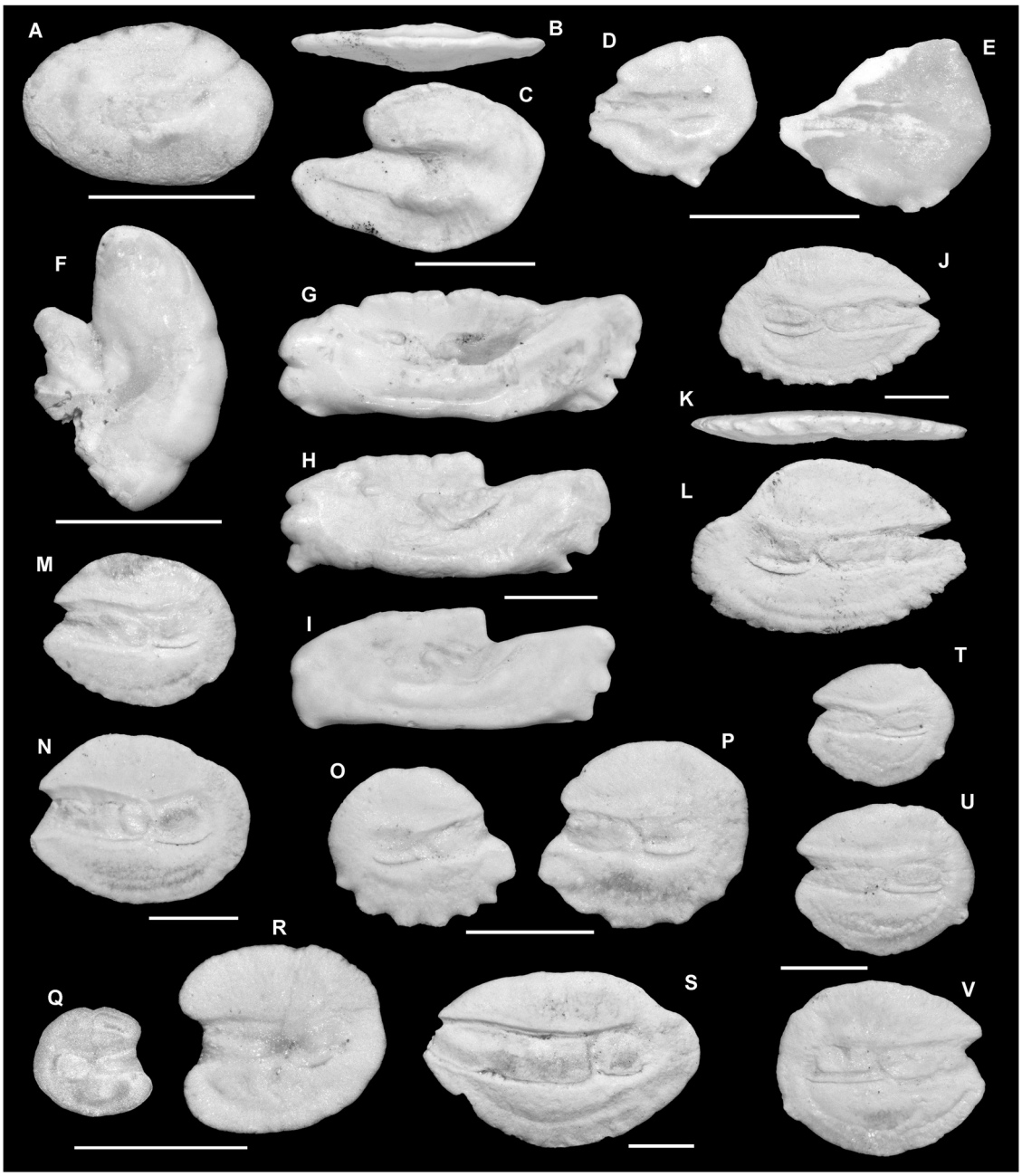

Fig. 10. Fish otoliths from the Red Sea sea bottoms. Pictures are inner views unless otherwise indicated. **A.** Congridae indet., M31/2-GKG 100-1 (393 m). **B, C.** Clupeidae indet., M31/2 (1040 m); B: ventral view. **D, E.** *Maurolicus* sp., M31/2-GKG 93-3 (685 m). **F.** *Ichthyococcus* sp., M5-85 (772–779 m). **G–I.** *Lestrolepis* sp.; G: M5-173 KG (431 m); H, I: M31/2-GKG 93-3 (685 m). **J–L.** *Diaphus coeruleus*; J: M31/2-GKG 93-3 (685 m); K, L: M5-183 Ku (2119–2120 m); K: ventral view. **M, N.** *Diaphus garmani*, M5-85 (772–779 m). **O, P.** *Diaphus arabicus*, M5-85 (772–779 m). **Q, R.** *Lampanyctus* sp., M5-85 (772–779 m). **S.** *Myctophum aurolaternatum*, M5-85 (772–779 m). **T–V.** *Benthosema pterotum*, M31/2-GKG 93-3 (685 m). Scale bars: 1 mm.

the same species. The otoliths are characterized by an elongate shape, with a blunt, but protruding rostrum in the center of the anterior rim and a dorsally extended and tapering posterior part. The dorsal rim is markedly undulated. The outline of the otoliths and the large ventral area resemble those of *Nezumia*, however, the 'pince-nez'-shaped sulcus with an upwardly bent crista superior, the less delimitated crista superior, and the convex inner face suggest a closer relationship with the genus *Coryphaenoides* than with *Nezumia*. Because no large comparative macrourid otoliths matching these specimens are available so far, they are only assigned to the family Macrouridae.

3.2. The Red Sea taxa

Order Stomiiformes Regan, 1909
Suborder Gonostomatoidei Weitzman, 1974
Family Sternoptychidae Dumeril, 1805
Subfamily Maurolicinae Gill, 1885
Genus ***Maurolicus*** Cocco, 1838
Maurolicus sp.
Fig. 10(D, E)

Remarks: These otoliths resemble much to those of *Maurolicus muelleri* (Gmelin, 1789), a cosmopolitan species that is frequently

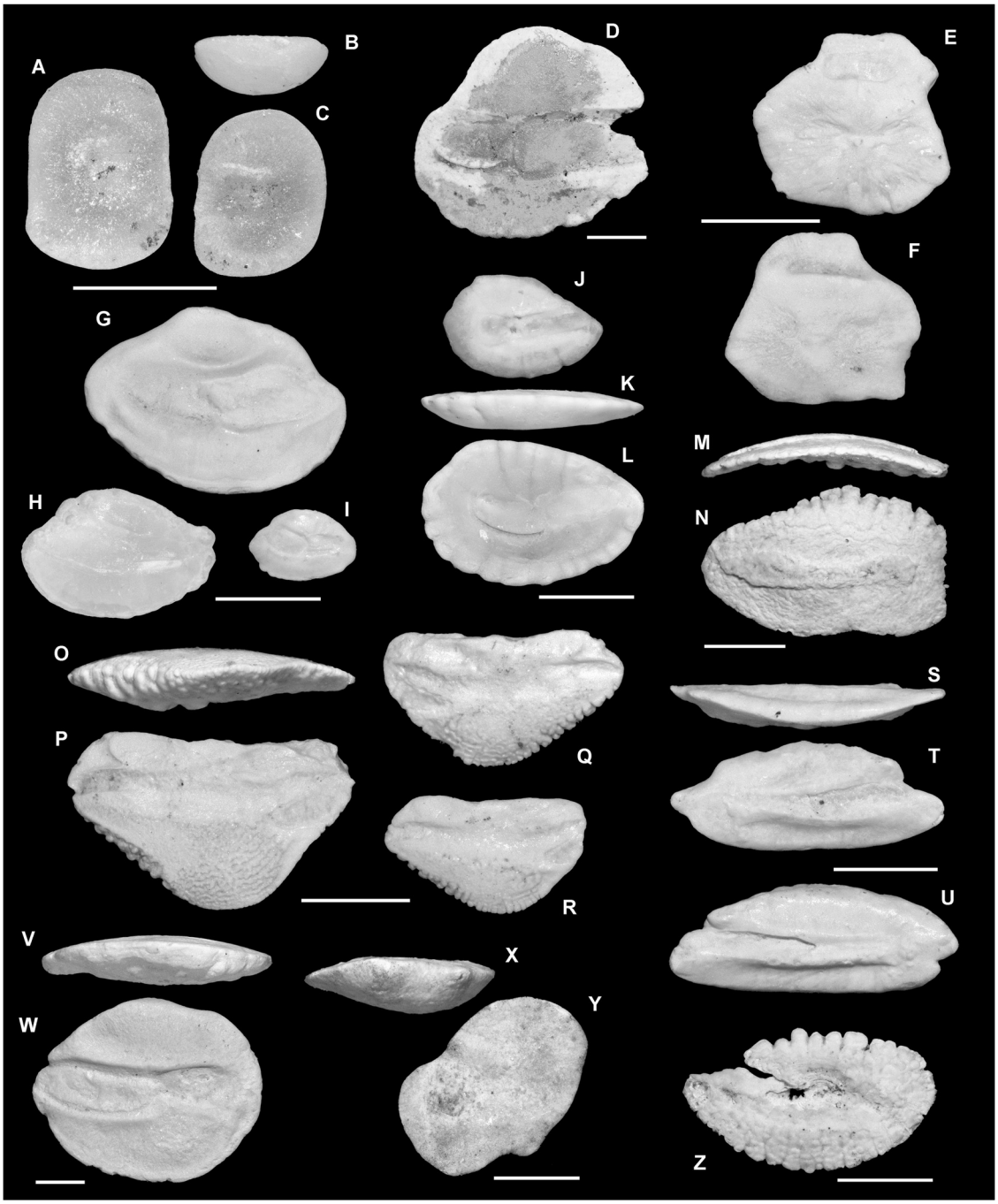

Fig. 11. Fish otoliths from the Red Sea sea bottoms. Pictures are inner views unless otherwise indicated. **A–C.** *Nannobrachium* sp., M5-85 (772–779 m); B: ventral view. **D.** *Diaphus ostenfeldi*, M5-85 (772–779 m). **E, F.** *Bregmaceros* sp., M31/2-GKG 93-3 (685 m). **G–I.** Apogonidae indet., M31/2-GKG 93-3 (685 m). **J–L.** *Lampadena luminosa*, M5-85 (772–779 m); K: ventral view. **M, N.** Hemiramphidae indet., M5-85 (772–779 m); M: ventral view. **O–R.** *Myripristis* sp.; O, P: M31/2-GKG 93-3 (685 m); Q, R: M5-183 Ku (2119–2120 m); O: ventral view. **S–U.** *Trichiurus* sp., M31/2-GKG 93-3 (685 m); S: ventral view. **V, W.** Myctophidae indet., M31/2-GKG 93-3 (685 m); V: ventral view. **X, Y.** *Hoplostethus* sp., M31/2 (1040 m); X: ventral view. **Z.** *Cubiceps* sp., M5-85 (772–779 m). Scale bars: 1 mm.

found in the sea bottoms of NE Atlantic and the central Mediterranean and also a well-known Recent species known as fossil from many Neogene and Quaternary localities. In their updated checklist of Red Sea fishes, Golani and Bogorodsky (2010) listed a single species of *Maurolicus*: *Maurolicus mucronatus* Klunzinger, 1871, and according to Parin and Kobyliansky (1993), all previous Red Sea records of *M. muelleri* are misidentification of *M. mucronatus*. Although it is very likely that our *Maurolicus* otoliths are those of *M. mucronatus*, yet the available otoliths of *M. mucronatus* (IRSNB collection) are of insufficient quality for an unambiguous assignment.

Suborder Phosichthyoidei Weitzman, 1974
Family Phosichthyidae Weitzman, 1974
Genus ***Ichthyococcus*** Bonaparte, 1840
Ichthyococcus sp.
Fig. 10(F)

Remarks: In the Red Sea checklist, Golani and Bogorodsky (2010) did not include any species of *Ichthyococcus*. Our otolith specimen shows the characteristic tall shape, with pointed ends at both the dorsal and ventral rims, which greatly resembles *Ichthyococcus ovatus* (Cocco, 1838), a circumglobal species that is also commonly found in the NE Atlantic and the central

Mediterranean samples (see Fig. 3(O, P), though both specimens are slightly broken at their anterior tips). The otoliths of other *Ichthyococcus* species from neighboring geographical areas, such as the Indian Ocean *Ichthyococcus parini* Mukhacheva, 1980, are not available so far for direct comparison. The occurrence of this single *Ichthyococcus* otolith suggests the potential presence of this genus in the Red Sea; however, any statement is yet tentative.

Order Aulopiformes Rosen, 1973
Suborder Alepisauroidei Regan, 1911
Family Lestidiidae Harry, 1953
Genus ***Lestrolepis*** Harry, 1953
Lestrolepis sp.
Fig. 10(G–I)

Remarks: Several paralepidid otoliths were recovered. They are characterized by a very elongate shape, a large ostial colliculum reaching to the antero-dorsal rim, and a swollen ventral area. They are highly similar to *Lestrolepis* otoliths (Smale et al., 1995: pl. 16, figs. C1, C2; Lin and Chang, 2012: pls. 9, 77), and all very likely belong to the same species. *Lestrolepis luetkeni* (Ege, 1933) is the only species known from the Red Sea (Golani and Bogorodsky, 2010); unfortunately, its otoliths have never been collected or figured in the literature.

Order Gadiformes Goodrich, 1909
Family Bregmacerotidae Gill, 1872
Genus ***Bregmaceros*** Thompson, 1840
Bregmaceros sp.
Fig. 11(E, F)

Remarks: The otoliths of *Bregmaceros* are very common in the sediment samples, but in most cases they are poorly preserved. As in the fossil specimens, they are easily distinguished from other gadiforms at the generic level, but identification at the species level is usually hazardous (Přikryl et al., 2016). *Bregmaceros arabicus* D'Ancona et Cavinato, 1965, is currently the single *Bregmaceros* that has been reported from the Red Sea (Golani and Bogorodsky, 2010), and it is very likely that all of our *Bregmaceros* otoliths belong to this species, but again, its otoliths have never been collected or figured in the literature for a comparative study.

Order Holocentriformes Betancur-R. et al., 2013
Family Holocentridae Bonaparte, 1833
Subfamily Myripristinae Nelson, 1955
Genus ***Myripristis*** Cuvier, 1829
Myripristis sp.
Fig. 11(O–R)

Remarks: Many *Myripristis* otoliths were found in deep-sea sediments (> 600 m). As with the otoliths of *Bregmaceros*, the heart-shaped otoliths of *Myripristis* (and other Myripristinae) are very distinctive but difficult to identify below the generic level (Lin and Chang, 2012: pls. 18, 19, 86, 87). Our *Myripristis* otoliths were all juvenile specimens with a slightly wider dorsal rim and a much shallower ventral area than any of the examined adult *Myripristis* specimens (IRSNB collection). These features are, however, somewhat closer to those of *Plectrypops lima* (Valenciennes, 1931) otoliths, which is an Indo-Pacific species (Smale et al., 1995: pl. 44, figs. B1, B2; Rivaton and Bourret, 1999: pl. 14, figs. 13, 14). The slight differences of otolith outline between our specimens and other large comparative *Myripristis* otoliths can be due to ontogeny, and although poorly preserved in most of our specimens, we judge the orientation of the ostium is more similar to that of *Myripristis*. Three species of *Myripristis* have been documented so far from the Red Sea, but *P. lima* has never been reported from this area (Golani and Bogorodsky, 2010).

Order Kurtiformes *sensu* Johnson, 1993
Family Apogonidae Günther, 1859
Apogonidae indet.
Fig. 11(G–I)

Remarks: Our apogonid otoliths show variations in the posterior rim and the relative size of the ostium, suggesting that more than one species may be involved. More than 50 species of cardinalfish have been documented from the Red Sea (Dor, 1984; Gon and Golani, 2002; Gon and Randall, 2003a, 2003b; Golani and Bogorodsky, 2010; Bogorodsky et al., 2014); however, the currently available otolith specimens of this group are far from sufficient for reliable identification at the species level. Furthermore, most of the apogonid otoliths only exhibit subtle interspecific differences (Lin and Chang, 2012: pls. 30–32, 98–100). Therefore, it is not our intention to emphasize much on the systematic assignment of these otoliths before a more comprehensive view of the apogonid otoliths is achieved.

Order Scombriformes Bleeker, 1859
Suborder Scombroidei Bleeker, 1859
Family Trichiuridae Rafinesque, 1815
Subfamily Trichiurinae Rafinesque, 1815
Genus ***Trichiurus*** Linnaeus, 1758
Trichiurus sp.
Fig. 11(S–U)

Remarks: Trichiurid otoliths are rare in the bottom sediments, either in the Red Sea or the NE Atlantic-Mediterranean area. In the Red Sea samples, four trichiurid otoliths have been recorded at station GKG 93-3 (685 m b.s.l.) and a single one at GKG 100-1 (393 m b.s.l.). These otoliths are identified here as *Trichiurus* sp. based on their sulcus, which is deeply incised in the anterior half of the otolith, and the swollen, elevated cristae that extend much more to the posterior part of the otolith. In addition, their outer face is strongly concave in the dorsoventral direction, and correspondingly, the inner face is convex only along the dorsoventral axis but flat in the anteroposterior direction. Golani and Bogorodsky (2010) recorded two species of *Trichiurus* in the Red Sea: *T. auriga* (Klunzinger, 1884) and *T. lepturus* (Linnaeus, 1758), but because there are no otolith specimens or illustrations available for *T. auriga*, our otoliths are provisionally assigned here to *Trichiurus* sp.

4. Results

4.1. Relative abundances in the Red Sea

Three pelagic taxa, namely *Maurolicus* sp., *Benthosema pterotum*, and *Bregmaceros* sp., were the dominant taxa in the Red Sea bottom sediments (Fig. 12; Table 2). Of these, *B. pterotum* was the most dominant, with an abundance exceeding 50% of the pelagic otoliths in most of the intervals (see below, Section 4.2). The pelagic otoliths showed the highest species richness in the 700–800 m interval. With respect to the abundance of benthic and benthopelagic taxa, a slightly more scattered pattern than that of the pelagic taxa was observed at different depth intervals, although only a total of five taxa were recorded. In fact, their abundance was extremely low (commonly less than five specimens in each interval), except for that in the richest 600–700 m interval, where 20 benthic and benthopelagic otoliths were found. Among these, apogonid otoliths were very common and abundant relative to others (Fig. 12). For the relative otolith abundance in the NE Atlantic and the Mediterranean samples, the reader is referred to Lin et al. (2016) and Lin et al. (2017b), respectively.

4.2. Diversity and richness

Simpson's diversity index was high in MMNEA, HNEA and CM regions, and otolith assemblages of CM and RS appeared to be

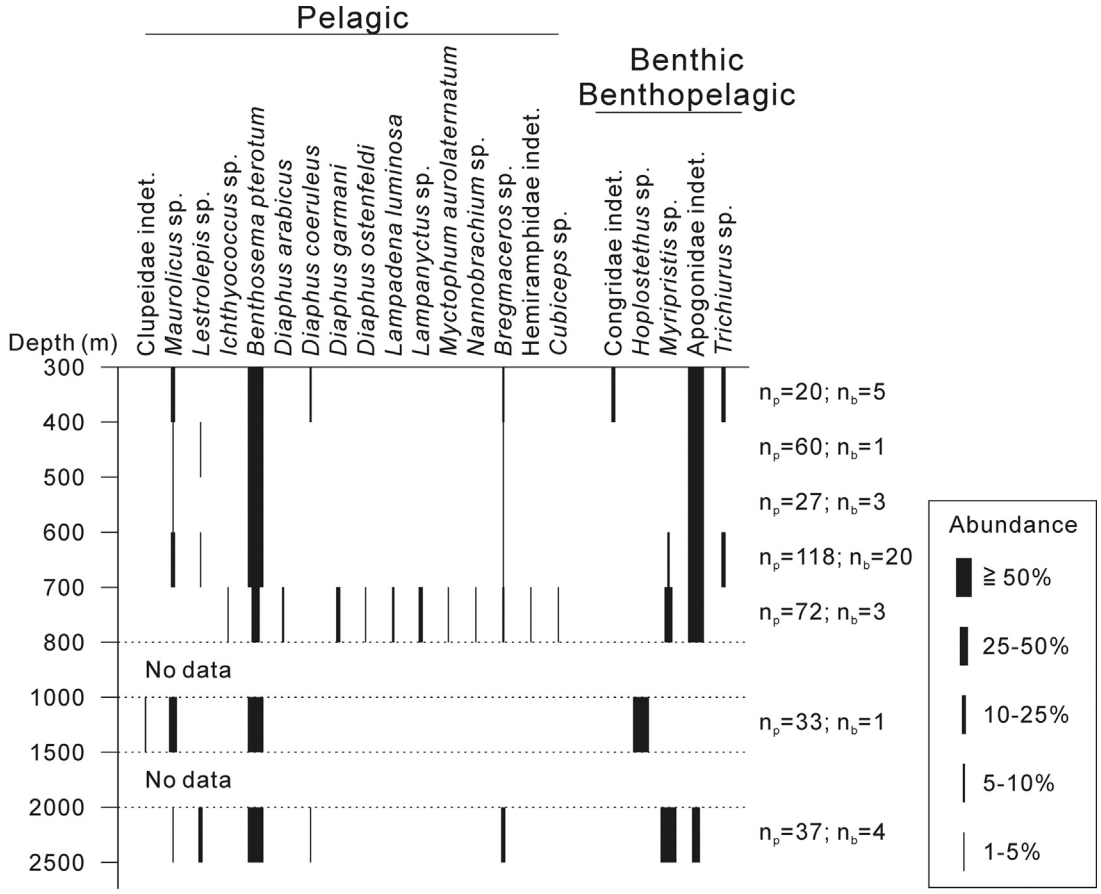

Fig. 12. Abundance of otolith taxa along a depth gradient in the Red Sea. Pelagic and benthic-benthopelagic taxa are considered separately in the analysis. The thickness of the vertical lines indicates the relative abundance; any taxon with relative abundance < 1% is not shown. The total number of identified otoliths is indicated for each depth interval and separated into pelagic (n_p) and benthic-benthopelagic (n_b) groups.

dominated by few taxa at depths < 500 m, as shown by Pielou's evenness index (Fig. 13). Higher variabilities were observed for both indices in CM at depths < 500 m. Finer (100 m) intervals reveal that the variabilities likely reflect smaller sample sizes at depths of 200–400 m (Fig. 13), but they might also imply heterogeneity in the taxonomic composition and abundance in this shallowest depth interval (see below).

Sample-based rarefaction and extrapolation curves showed that with sufficient sampling, the number of taxa might be expected to be more than twice as observed at depths 500–1000 m for CM, MNEA, and RS, but might not increase drastically at deeper and shallower depths (Fig. 14). Interestingly, the rarefaction and extrapolation curves estimate the highest number of taxa in the mid-depth samples compared to samples at shallower or deeper depths (Fig. 14).

Since a more continuous depth range was available for CM samples than for other regions, we compared their diversity and richness along a 500 m-interval depth gradient. The values of Simpson's diversity index were rather stable along the depth gradient, ranging between 0.8 and 0.9 (Fig. 13). On the other hand, rarefaction and extrapolation curves revealed that approximately 30–40 taxa can be expected at depths < 400 m, 50–60 taxa at depths 400–500 m, > 60 taxa at depths 1000–1500 m, and 20 taxa at depths > 2000 m. The large 95% confidence interval at depths 500–1000 m did not allow an unambiguous interpretation. As a result, taxa count likely peaked at depths 1000–1500 m and dropped quickly in deeper sediments (Fig. 14).

4.3. Comparison of assemblages

Cluster analysis based on taxonomic composition generally grouped stations according to their geographical origin (Fig. 15). The NS, RS, and HNEA (except for a single RS and two HNEA unresolved stations) otolith assemblages formed well-defined clusters, whereas those of CM and MNEA were grouped together. Similarly, PCoA reveals that a certain biogeographical continuity was evident between CM and MNEA, while NS, RS, and HNEA were clearly separated in the multidimensional space (Fig. 16).

ANOSIM analysis was performed at < 500 m and 500–1000 m depth intervals for CM, MNEA, and HNEA (Figs. 15 and 16). It indicated that each region is structured by a specific combination of taxa (Global R = 0.402, p = 0.003, and Global R = 0.616, p = 0.001, respectively). Pairwise comparison by SIMPER analysis further revealed a rather high dissimilarity between CM and MNEA (Overall Average Difference δi = 0.836; Table 3) in the < 500 m depth interval (no HNEA samples are available for this shallow interval). In the 500–1000 m depth interval, high dissimilarity values were also obtained for CM-HNEA (δi = 0.873) and MNEA-HNEA (δi = 0.880), whereas it was lower for CM-MNEA (δi = 0.683) (Table 3). In all cases, the otolith abundance of mesopelagic fishes greatly contributed to the SIMPER result: at depths < 500 m, the otolith abundance of *Maurolicus muelleri* and *Hygophum benoiti* defined the CM region, and *Ceratoscopelus* spp. and *Cubiceps gracilis* defined the MNEA region. At depths 500–1000 m, *Hygophum benoiti* and *H. hygomii* dominated the CM region, whereas

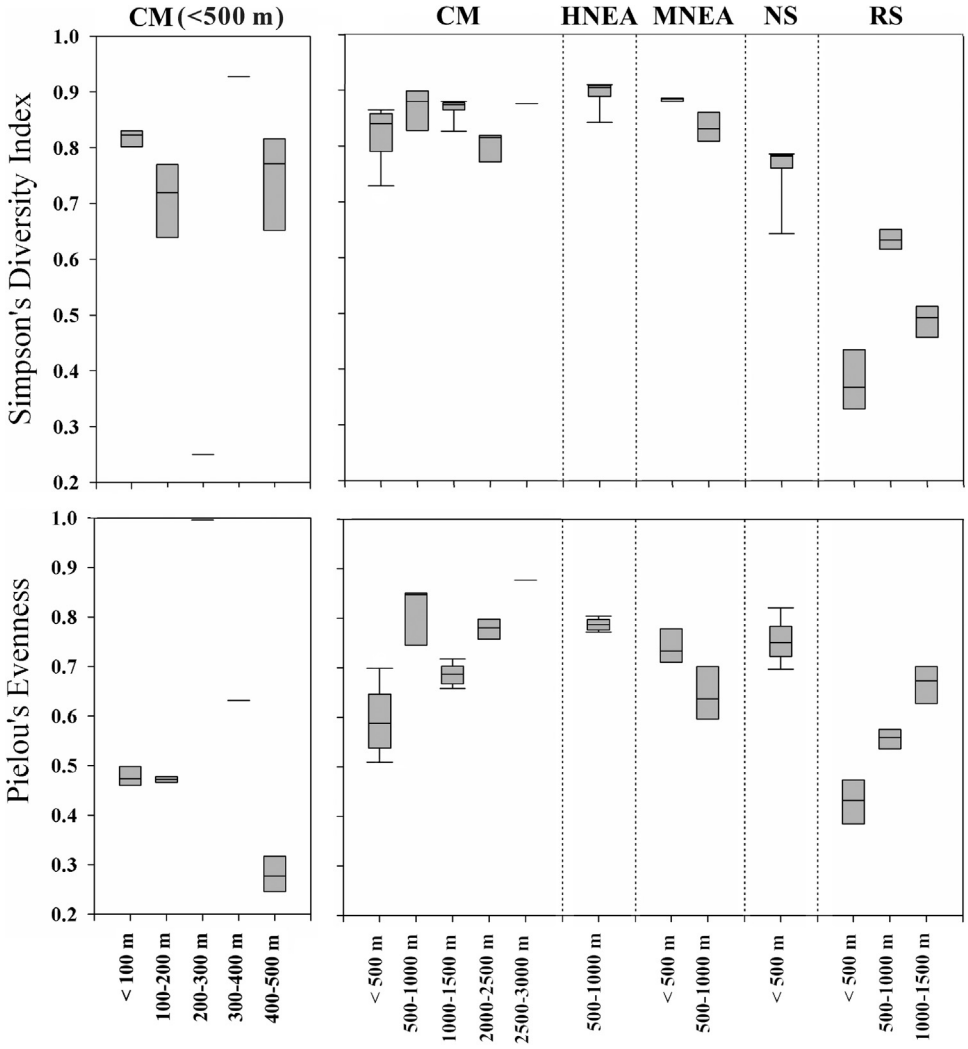

Fig. 13. Otolith assemblages from different region show differences in Simpson's diversity and Pielou's evenness indices. Samples are grouped into finer 100 m-depth intervals in CM and into 500 m intervals for all regions for comparison. Note that the value of Pielou's evenness for 200–300 m depth in CM is close to 1. CM: central Mediterranean; HNEA: high-latitude NE Atlantic; MNEA: middle-latitude NE Atlantic; NS: North Sea; RS: Red Sea.

Ceratoscopelus maderensis and *Electrona risso* defined the MNEA region, and *Benthosema glaciale* and *Scopelogadus beanii* the HNEA region (Table 3).

Differences in the composition of the CM samples for each 500 m-depth interval were not detected by ANOSIM (Global $R = -0.00268$, $p = 0.602$; negative R suggests higher similarity between than within depth intervals), instead, a slightly better separation of assemblages along the depth gradient was observed when samples at depths < 500 m were assigned into 100 m-depth intervals and samples > 1000 m into a single group (Global $R = 0.2873$, $p = 0.001$). SIMPER analysis suggested that *Maurolicus muelleri* is an important species for indicating shallow assemblages, but many mesopelagic taxa are more or less equally contributing to the dissimilarity measure for deeper assemblages (Appendix D). Therefore, the otolith composition of our CM samples was not strictly depth-structured.

5. Discussion

5.1. Taxonomic evaluation

The occurrences of otolith taxa in the bottom sediments strongly resemble their Present geographical distribution (Lin et al., 2016, 2017b; Table 2), except that of the presence of *Protomyctophum arcticum* otoliths found in CM samples. *Protomyctophum arcticum* is a subpolar to temperate North Atlantic species, which is unknown in the present-day Mediterranean. However, their occurrence in the late Pleistocene Mediterranean is supported by other dredge sediments from the Tyrrhenian Sea (central Mediterranean) (Girone et al., 2006). Therefore, it is likely that part of our otolith assemblages also represents components of a slightly older (late Pleistocene) association, though according to Lin et al. (2017b), the majority of the assemblages are likely to represent the most recently dead association.

Otolith assemblages from RS reflect a poorly diversified regional community strongly dominated by very few taxa. The abundance and diversity of the pelagic taxa are much higher than those of the benthic-benthopelagic taxa (Fig. 12), resembling the results obtained from the NE Atlantic (Lin et al., 2016) and the Mediterranean samples (Lin et al., 2017b). More diverse and different assemblages are expected to be found at shallower depths. A detailed and conclusive taxonomic interpretation, however, requires a more comprehensive knowledge of Recent otoliths of this realm (RS and the Western Indian Ocean in general). Relevant regional otolith monographs such as Smale et al. (1995) on the fishes of South African seas and Rivaton and Bourret (1999) on those from the Indo-Pacific Ocean are

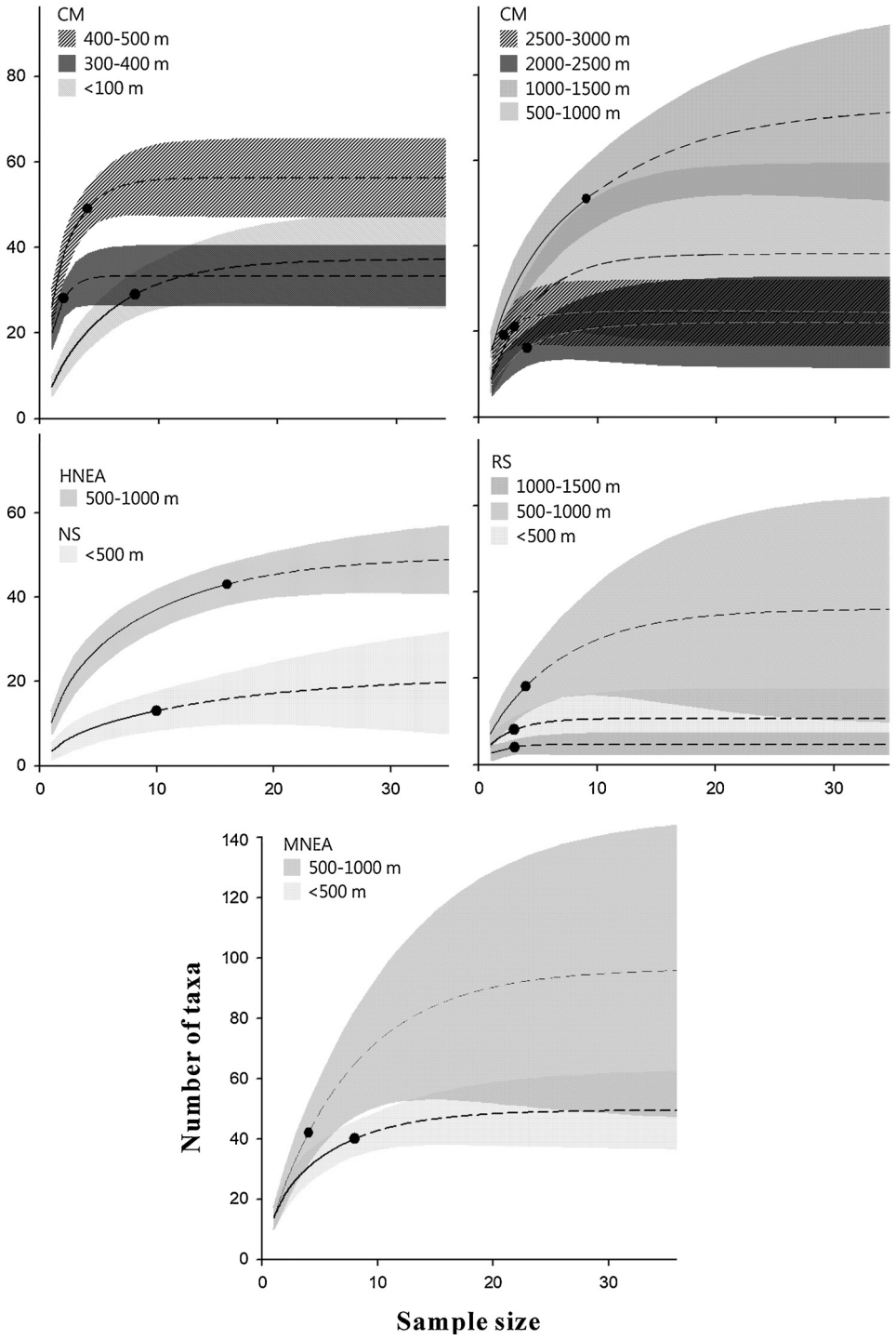

Fig. 14. Sample-based rarefaction and extrapolation curves with their 95% confidence intervals. Samples are grouped into depth intervals. Reference samples are indicated by solid circles, average rarefaction by solid lines, and average extrapolation by dashed lines. Depth intervals with less than two samples were not plotted. CM: central Mediterranean; HNEA: high-latitude NE Atlantic; MNEA: middle-latitude NE Atlantic; NS: North Sea; RS: Red Sea.

insufficient for a reliable assignment of many of our specimens. Consequently, a more extensive otolith collection from RS and southern Arabia is needed to solve many taxonomic issues. In their updated checklist, Golani and Bogorodsky (2010) listed the presence of only two myctophids, namely *Benthosema pterotum* and a single *Diaphus* species, *Diaphus coeruleus* (Klunzinger, 1871) in the Red Sea. Interestingly, our RS material reveals the occurrence of three additional *Diaphus* species in the bottom sediments, namely *D. arabicus* Nafpaktitis, 1978 (Fig. 10(O, P)), *D. garmani* Gilbert, 1906 (Fig. 10(M, N)), and *D. ostenfeldi* Tåning, 1932 (Fig. 11(D)) (see also Schwarzhans, 2013b for illustrations), all having their Modern distribution in the Western Indian Ocean. This could, in part, result from the mixing of older (late Pleistocene) material, as discussed earlier. The presence of additional myctophid species might be related to different environmental conditions in the past. However, the possibility that more myctophid species may exist in the Modern Red Sea could not be totally excluded.

Otoliths of several shallow-water taxa such as apogonids and myripristids were, however, found frequently in the sediments at depths greater than 500 m b.s.l. (Fig. 12). These shorefishes inhabit

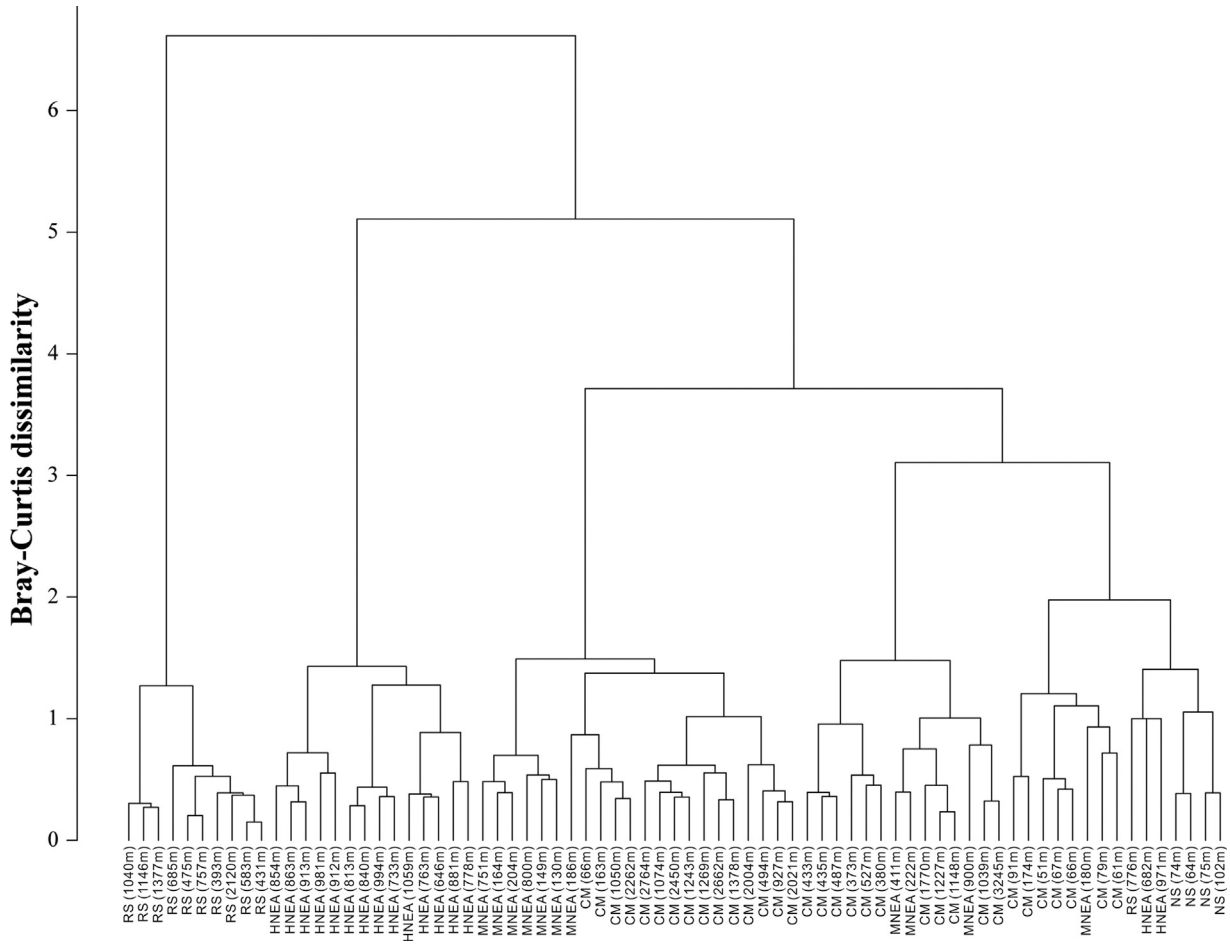

Fig. 15. Dendrogram based on the composition (absolute abundances) of each station (coded by region and average sampling depth). Hierarchical cluster analysis achieved using Ward algorithm and the square-rooted Bray-Curtis dissimilarity index. CM: central Mediterranean; HNEA: high-latitude NE Atlantic; MNEA: middle-latitude NE Atlantic; NS: North Sea; RS: Red Sea. See Appendices A–C for compositional details for each sample.

shallow water up to a depth of 100 m, rarely over 200 m (Nelson et al., 2016), making their otolith occurrence in deep-water sediments worth noting. Although it remains difficult to interpret such occurrences, the steep bottom topography in RS (Braithwaite, 1987) could be one important reason why mixing of shallow and deep sediments is prone to happen here. The cases of apogonids and myripristids, together with myctophids, clearly suggest that more work are required to explore the gap between living fish communities and dead assemblages in the sediments.

In contrast to the Red Sea region, the well-established Recent otolith collections (e.g., the IRSNB collection) and many published otolith illustrations (Tuset et al., 2008; Nolf, 2013) facilitated the identification of MNEA, HNEA and CM otoliths. Nevertheless, otoliths of several taxa such as the alepocephalids remain poorly known, and complete otolith growth series of many species are still lacking. This study unveils otoliths of several taxa that are commonly found in the sediments but have received little attention so far. In addition, otolith ontogenetic change in many species was highlighted, an information which is often lacking in the otolith collections and/or published illustrations.

5.2. Diversity and richness

The diversity index in CM, MNEA, and HNEA are generally higher than those of RS and NS (Fig. 13), although this can simply be attributed to sample size differences. The rarefaction and extrapolation curves point toward highest taxonomic richness at mid-water depths (i.e., at 500–1000 m depths in MNEA, HNEA and RS, and 1000–1500 m in CM; Fig. 14). As detailed by CM samples, the otolith richness is higher at depths < 500 m than at depths > 2000 m, but both are lower than at 1000–1500 m b.s.l. This relationship between species richness and depth does not entirely agree with the Modern fish communities, where a decreasing richness pattern is observed from shallow to greater depths (Cartes et al., 2004; D'Onghia et al., 2004; Mytilineou et al., 2005; Menezes et al., 2006; Danovaro et al., 2010; Follesa et al., 2011; Farré et al., 2016); it does not perfectly support the statement that higher otolith richness can be observed in the sediments at depths < 500 m in CM (Lin et al., 2017b). Richness at deeper intervals (> 500 m) likely represent true richness as in the fish communities: the mid- and deep-water sediments, where otoliths were buried in calmer and stable settings, obviously provide a more suitable environment for otolith preservation than those of shallow waters. These results may imply that there is a preferential preservation at mid-water depth. Mechanical water current and bioturbation in the shallow environment might be some of the reasons impeding burial (Wigley and Stinton, 1973; Nolf, 1985; Schwarzhans, 2013a; Lin et al., 2017b). Richness and abundance heterogeneity among shallow assemblages is obvious, due to a more fragmented distribution of otoliths (Lin et al., 2017b: fig. 3; Fig. 13). Wigley and Stinton (1973) reported more diverse shallow water otolith assemblages from the western Atlantic, but lacking sufficient deeper assemblages for comparison. On the other hand, larger sample size in CM and/or NEA at shallower depths would be helpful for our interpretation.

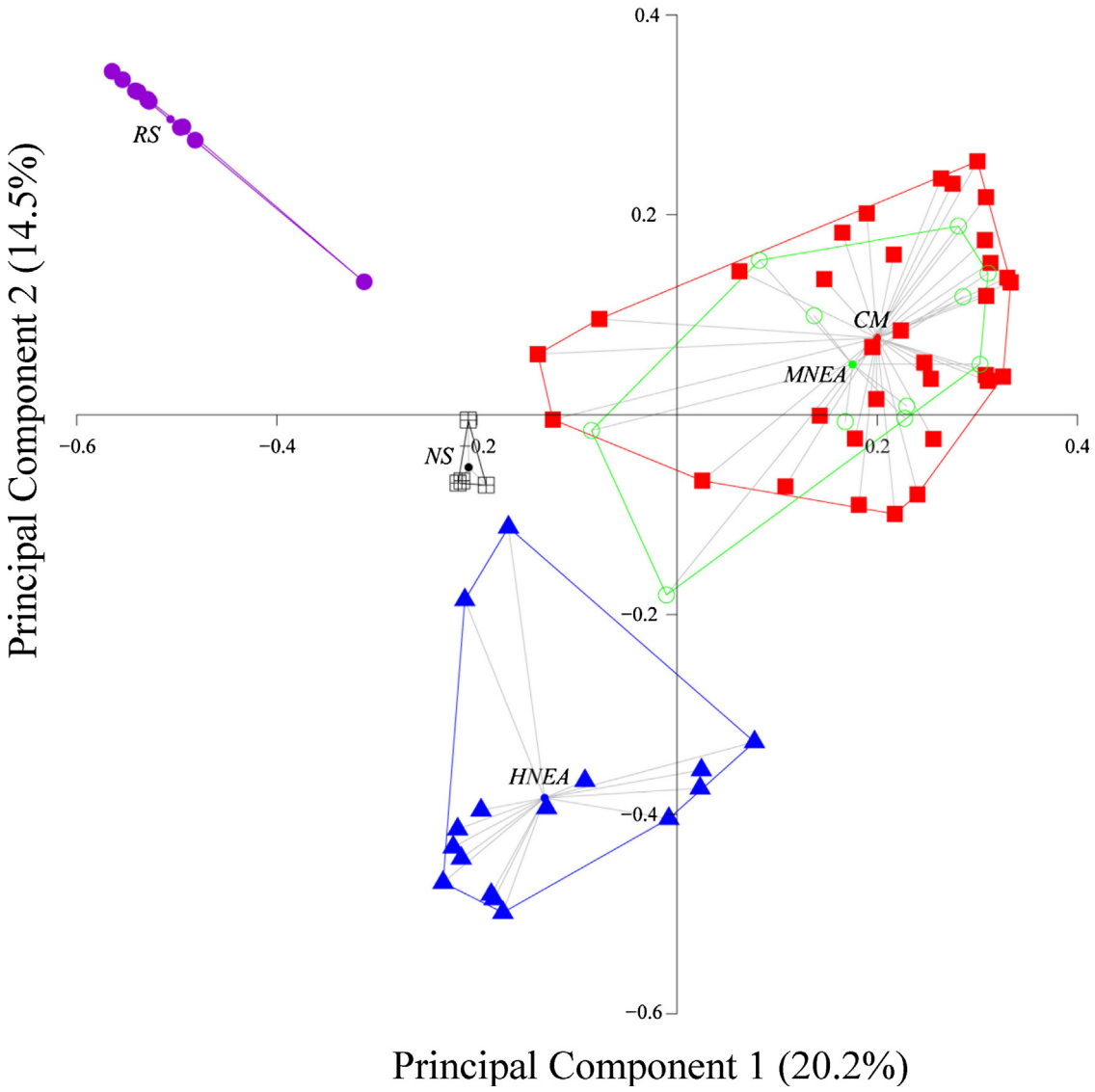

Fig. 16. First two dimensions of a principal coordinate analysis (PCoA, with centroid distances) on the composition (absolute abundances) of each station based on the square-rooted Bray-Curtis dissimilarity matrix. CM: central Mediterranean; HNEA: high-latitude NE Atlantic; MNEA: middle-latitude NE Atlantic; NS: North Sea; RS: Red Sea.

5.3. Similarities and differences among assemblages

The taxonomic composition of the otolith assemblages varies from location to location; it is strongly related to Present distribution of the taxa and post-mortem transportation is not evident (Lin et al., 2016). A clear separation among regional assemblages corroborates this statement (Figs. 15, 16), showing that each region is defined by a characteristic combination of taxa. As a consequence, given a sample of unknown sampling location, its composition and abundance in otolith taxa will likely determine its origin, at least in the present study area (Lin et al., 2016). An exception comes from a certain compositional continuity between CM and MNEA assemblages at greater depths (Figs. 15, 16), where pelagic taxa account for the majority of common taxa that resulted in the grouping structure evidenced by cluster analysis and PCoA. The species composition of our otolith assemblages thus reflects the regional fish fauna and, as expected, samples from CM share many taxa with the NE Atlantic but not with RS.

The assemblages were, however, not strictly depth-structured in CM. Compositions are clearly more heterogeneous at depths < 500 m b.s.l. (see above, Section 5.2.), but at depths below 1000 m, the assemblages are nearly identical (Lin et al., 2017b; Appendix D). Thus, separating and defining each depth interval is still challenging at the moment. Nevertheless, a sharp difference does exist at *ca.* 500 m b.s.l. (see also Lin et al., 2017b: fig. 6), and a more comprehensive pattern might be resolved with sufficient shallow water samplings at finer depth intervals because more indicative taxa would be expected there, as in the living fish communities.

5.4. Application to fossil assemblages

Apart from comparing the otolith thanatocoenoses and fish biocoenoses, it is noteworthy to evaluate them with fossil assemblages. Interestingly, few taxa are common or even abundant in the Modern Mediterranean and fossil localities but have not been documented so far in any of the NE Atlantic and Mediterranean sediments. For example, abundant fossil otoliths of *Hoplostethus* have been reported from the Tortonian of northern Italy (Lin et al., 2015, 2017a), and otoliths of *Hoplostethus mediterraneus* Cuvier, 1829, a NE Atlantic and Mediterranean common species, have also been reported from the Pleistocene of Italy (Girone et al., 2006, as *Hoplostethus* cf. *mediterraneus*), but *Hoplostethus* otoliths have not been found in the Modern

Table 3
Results of the SIMPER analyses between each region at < 500 m and 500–1000 m depths, listing the ten first taxa in decreasing order of contribution to the overall average dissimilarity (δi within parenthesis; δi for each taxon represents its average contribution to the overall average dissimilarity; sd: standard deviation).

CM-MNEA, < 500 m (δi = 0.836)			HNEA-MNEA, 500–1000 m (δi = 0.880)		
Taxa	δi	sd	Taxa	δi	sd
Maurolicus muelleri	0.0726	0.0678	*Ceratoscopelus maderensis*	0.0856	0.0467
Hygophum benoiti	0.0539	0.0391	*Electrona risso*	0.0723	0.0381
Ceratoscopelus maderensis	0.0474	0.0359	*Scopelogadus beanii*	0.0410	0.0305
Cubiceps gracilis	0.0450	0.0342	*Myctophum punctatum*	0.0358	0.0123
Hygophum hygomii	0.0434	0.0368	*Lampanyctus crocodilus*	0.0328	0.0232
Ceratoscopelus warmingii	0.0425	0.0530	*Hygophum benoiti*	0.0325	0.0309
Scopelarchus analis	0.0392	0.0262	*Hygophum hygomii*	0.0325	0.0309
Gobiidae indet.	0.0390	0.0395	*Benthosema glaciale*	0.0290	0.0279
Electrona risso	0.0359	0.0265	*Lobianchia dofleini*	0.0286	0.0242
Lobianchia dofleini	0.0280	0.0274	*Micromesisteus poutassou*	0.0282	0.0291
CM-HNEA, 500–1000 m (δi = 0.873)			CM-MNEA, 500–1000 m (δi = 0.683)		
Taxa	δi	sd	Taxa	δi	sd
Hygophum benoiti	0.0814	0.0260	*Electrona risso*	0.0469	0.0392
Scopelogadus beanii	0.0643	0.0352	*Ceratoscopelus maderensis*	0.0445	0.0537
Ceratoscopelus maderensis	0.0596	0.0268	*Myctophum punctatum*	0.0343	0.0092
Hygophum hygomii	0.0467	0.0258	*Benthosema glaciale*	0.0313	0.0235
Electrona risso	0.0451	0.0268	*Hygophum benoiti*	0.0286	0.0201
Benthosema glaciale	0.0359	0.0246	*Maurolicus muelleri*	0.0242	0.0289
Lampanyctus macdonaldi	0.0342	0.0343	*Scopelarchus analis*	0.0222	0.0193
Maurolicus muelleri	0.0331	0.0353	*Protomyctophum arcticum*	0.0200	0.0216
Lampanyctus crocodilus	0.0319	0.0270	*Opisthoproctus soleatus*	0.0194	0.0301
Bathylagus euryops	0.0312	0.0385	*Hygophum hygomii*	0.0192	0.0144

CM: central Mediterranean; HNEA: high-latitude NE Atlantic; MNEA: middle-latitude NE Atlantic; NS: North Sea; RS: Red Sea.

sediments of these regions. A single juvenile *Hoplostethus* otolith was found in RS sample (Fig. 11(X, Y)), but this is merely the only record thus far. *Hoplostethus* is generally a benthopelagic fish inhibiting the upper to middle slope (Whitehead et al., 1986–1989), a depth interval that is particularly challenging for paleoecological reconstruction based on fossil otoliths because of the coexistence of the shallow taxa (Lin et al., 2016, 2017b). If *Hoplostethus* otoliths were confidently recovered from the bottom sediments at such mid-water depths, their fossil occurrence could provide additional information signaling an upper to middle slope paleoenvironment.

6. Conclusions

The otoliths in sea bottom sediments are indeed widely distributed and their abundance and taxonomic resolution allow comparisons at the community scale. The richness of otolith taxa was highest at mid-water depths and the assemblages were geographically structured, despite a higher affinity between MNEA and CM regions at deeper depths. Depth-related assemblage composition was, however, not obvious in CM due to lower sample size in heterogeneous shallow waters and high affinity in the composition at greater depths. We found ecologically meaningful results with the first diversity assessments of these otolith assemblages, and expect similar results on the fossil material. However, further validation on the otolith assemblages and related fish communities and associated research would be helpful, including age confirmation of the otolith fossilization, inquiry into post-mortem transportation of the otolith, and sea-bottom assemblage exploration from other regions of the world. In addition to the diversity measures, our comprehensive taxonomic work would be especially helpful for identifying Plio-Pleistocene otoliths from the same region and in other fields such as identification of otoliths in the stomach contents of piscivores.

Acknowledgments

We thank André Freiwald (Wilhelmshaven) and Bettina Reichenbacher (München) for providing NE Atlantic material, Marco Taviani and Lorenzo Angeletti (ISMAR-CNR, Bologna) for providing the central Mediterranean Sea bottom sediment samples, and Kristiaan Hoedemakers (IRSNB) and Arie Janssen (Naturalis Biodiversity Center, Leiden) for the Red Sea otoliths. Dirk Nolf (IRSNB) is thanked for advising the systematics part. Very constructive and helpful comments on the statistical techniques were provided by the editor of the journal. Comments from two anonymous reviewers improved our manuscript. We are grateful to Katie Griswold (Smithsonian Tropical Research Institute, Panama) for improving the English. Chien-Hsiang Lin was financially supported by the Ministry of Education, Taiwan, under the title "Government scholarship for overseas study" during his Ph.D. studies. The microscope laboratory at the Dipartimento di Scienze della Terra and Geoambientali, University of Bari Aldo Moro was funded by Potenziamento Strutturale PONa3_00369 "Laboratorio per lo Sviluppo Integrato delle Scienze e delle Tecnologie dei Materiali Avanzati e per dispositivi innovativi (SISTEMA)".

Appendices A–D. Supplementary information

Supplementary information (including depth, coordinates and composition of sample from the NE Atlantic, central Mediterranean and Red Sea, and detailed results of SIMPER analyses) associated with this article can be found, in the online version, at: https://doi.org/10.1016/j.geobios.2018.06.002.

References

Almada, V.C., Oliveira, R.F., Goncalves, E.J., Almeida, A.J., Santos, R.S., Wirtz, P., 2001. Patterns of diversity of the north-eastern Atlantic blennid fish fauna (Pisces: Blenniidae). Global Ecology and Biogeography 10, 411–422.

Ben-Tuvia, A., 1964. Two siganid fishes of Red Sea origin in the eastern Mediterranean. Bulletin of the Sea Fisheries Research Station. Haif 37, 3–9.
Ben-Tuvia, A., 1966. Red Sea fishes recently found in the Mediterranean. Copeia 2, 254–275.
Bianchi, C.N., Morri, C., Chiantore, M., Montefalcone, M., Parravicini, V., Rovere, A., 2012. Mediterranean Sea biodiversity between the legacy from the past and a future of change. In: Stambler, N. (Ed.), Life in the Mediterranean Sea: a look at habitat changes. Nova Science Publishers, New York, pp. 1–60.
Bogorodsky, S.V., Alpermann, T.J., Mal, A.O., Gabr, M.H., 2014. Survey of demersal fishes from southern Saudi Arabia, with five new records for the Red Sea. Zootaxa 3852, 401–437.
Braithwaite, C.J.R., 1987. Geology and Palaeogeography of the Red Sea Region. In: Edwards, A.J., Head, S.M. (Eds.), Red Sea. Pergamon Press, Oxford, pp. 22–44.
Brzobohatý, R., Nolf, D., 1996. Otolithes de myctophidés (poissons téléostéens) des terrains tertiaires d'Europe: révision des genres *Benthosema, Hygophum, Lampadena, Notoscopelus* et *Symbolophorus*. Bulletin de l'Institut royal des Sciences naturelles de Belgique, Sciences de la Terre 66, 151–176.
Brzobohatý, R., Nolf, D., 2000. Diaphus otoliths from the European Neogene (Myctophidae, Teleostei). Bulletin de l'Institut royal des Sciences naturelles de Belgique, Sciences de la Terre 70, 185–206.
Cartes, J.E., Maynou, F., Moranta, J., Massutí, E., Lloris, D., Morales-Nin, B., 2004. Patterns of bathymetric distribution among deep-sea fauna at local spatial scale: comparison of mainland vs. insular areas. Progress in Oceanography 60, 29–45.
Clarke, K.R., 1993. Non-parametric multivariate analyses of changes in community structure. Australian Journal of Ecology 18, 117–143.
Colwell, R.K., 2013. EstimateS: Statistical estimation of species richness and shared species from samples. Version 9. User's Guide and application published at: http://purl.oclc.org/estimates.
Danovaro, R., Company, J.B., Corinaldesi, C., D'Onghia, G., Galil, B.S., Gambi, C., Gooday, A.J., Lampadariou, N., Luna, G.M., Morigi, C., Olu, K., Polymenakou, P., Ramírez-Llodra, E., Sabbatini, A., Sardà, F., Sibuet, M., Tselepides, A., 2010. Deep-sea biodiversity in the Mediterranean Sea: the known, the unknown, and the unknowable. PLoS One 5, e11832.
DiBattista, J.D., Berumen, M.L., Gaither, M.R., Rocha, L.A., Eble, J.A., Choat, J.H., Craig, M.T., Skillings, D.J., Bowen, B.W., 2013. After continents divide: comparative phylogeography of reef fishes from the Red Sea and Indian Ocean. Journal of Biogeography 40, 1170–1181.
Domingues, V.S., Bucciarelli, G., Almada, V.C., Bernardi, G., 2005. Historical colonization and demography of the Mediterranean damselfish *Chromis chromis*. Molecular Ecology 14, 4051–4063.
D'Onghia, G., Lloris, D., Politou, C.-Y., Sion, L., Dokos, J., 2004. New records of deep-water teleost fishes in the Balearic Sea and Ionian Sea (Mediterranean Sea). Scientia Marina 68, 171–183.
Dor, M., 1984. CLOFRES: Checklist of the Fishes of the Red Sea. The Israel Academy of Sciences and Humanities, Jerusalem.
Emig, C.C., Geistdoerfer, P., 2004. The Mediterranean deep-sea fauna: historical evolution, bathymetric variations and geographical changes. Carnets de Géologie 2004, 1–10.
Farré, M., Tuset, V.M., Cartes, J.E., Massutí, E., Lombarte, A., 2016. Depth-related trends in morphological and functional diversity of demersal fish assemblages in the western Mediterranean Sea. Progress in Oceanography 147, 22–37.
Follesa, M.C., Porcu, C., Cabiddu, S., Mulas, A., Deiana, A.M., Cau, A., 2011. Deep-water fish assemblages in the central-western Mediterranean (south Sardinian deep-waters). Journal of Applied Ichthyology 27, 129–135.
Galil, B.S., 2000. A sea under siege – alien species in the Mediterranean. Biological Invasions 2, 77–186.
García-Mederos, A.M., Tuya, F., Tuset, V.M., 2015. The structure of a nearshore fish assemblage at an oceanic island: insight from small scale fisheries through bottom traps at Gran Canary Island (Canary Islands, eastern Atlantic). Aquatic Living Resources 28, 1–10.
Gaudant, J., 2002. La crise messinienne et ses effets sur l'ichthyofaune néogène de la Méditerranée: le témoignage des squelettes en connexion de poissons téléostéens. Geodiversitas 24, 691–710.
Girone, A., 2003. The Pleistocene bathyal teleostean fauna of Archi (southern Italy): palaeoecological and palaeobiogeographic implications. Rivista Italiana di Paleontologia e Stratigrafia 109, 99–110.
Girone, A., 2005. Response of otolith assemblages to sea level fluctuations at the Lower Pleistocene Montalbano Jonico section (southern Italy). Bollettino della Società Paleontologica Italiana 44, 35–45.
Girone, A., 2007. Piacenzian otolith assemblages from northern Italy (Rio Merli section Emilia Romagna). Bollettino della Società Paleontologica Italiana 45, 159–170.
Girone, A., Nolf, D., Cappetta, H., 2006. Pleistocene fish otoliths from the Mediterranean Bas a synthesis. Geobios 39, 651–671.
Girone, A., Nolf, D., Cavallo, O., 2010. Fish otoliths from the pre-evaporitic (Early Messinian) sediments of northern Italy: their stratigraphic and palaeobiogeographic significance. Facies 56, 399–432.
Golani, D., Bogorodsky, S.V., 2010. The Fishes of the Red Sea—Reappraisal and Updated Checklist. Zootaxa 2463, 1–135.
Gon, O., Golani, D., 2002. A new species of the cardinalfish genus *Gymnapogon* (Perciformes Apogonidae) from the Red Sea. Ichthyological Research 49, 346–349.
Gon, O., Randall, J.E., 2003a. A review of the cardinalfishes (Perciformes: Apogonidae) of the Red Sea. Smithiana Bulletin 1, 1–46.
Gon, O., Randall, J.E., 2003b. Revision of the Indo-Pacific Cardinalfishes genus *Archamia* (Perciformes: Apogonidae) with description of a new species. Indo-Pacific Fishes 35, 1–49.
Goren, M., Galil, B.S., 2005. A review of changes in the fish assemblages of Levantine Inland and marine ecosystems following the introduction of non-native fishes. Journal of Applied Ichthyology 21, 364–370.
Gotelli, N.J., Colwell, R.K., 2011. Estimating species richness. In: Magurran, A.E., McGill, B.J. (Eds.), Frontiers in Measuring Biodiversity. Oxford University Press, New York, pp. 39–54.
Hammer, O., Harper, D.A.T., Ryan, P.D., 2001. PAST: paleontological statistics software package for education and data analysis. Paleontologica Electronica 4, 9.
Janssen, A., 2007. Holoplanktonic Mollusca (Gastropoda) from the Gulf of Aqaba Red Sea and Gulf of Aden (Late Holocene-Recent). Veliger 49, 140–195.
Laptikhovsky, V.V., Barrett, C.J., Hollyman, P.R., 2018. From coral reefs to whale teeth: estimating mortality from natural accumulations of skeletal materials. Marine Ecology Progress Series 598, 273–291, http://dx.doi.org/10.3354/meps12260.
Layman, C.A., Winemiller, K.O., 2005. Patterns of habitat segregation among large fishes in a Venezuelan floodplain river. Neotropical Ichthyology 3, 111–117.
Legendre, P., Anderson, M.J., 1999. Distance-based redundancy analysis: testing multispecies responses in multifactorial ecological experiments. Ecological Monographs 69 (1), 1–24.
Lin, C.-H., 2016. Fish otolith assemblages in Recent sea bottoms and in ancient (Eocene and Miocene) fossiliferous deposits: a comparative study of taxonomy and paleoecology. Ph.D. Thesis, Università degli Studi di Bari Aldo Moro. (unpubl.) .
Lin, C.-H., Brzobohatý, R., Nolf, D., Girone, A., 2017a. Tortonian teleost otoliths from northern Italy: taxonomic synthesis and stratigraphic significance. European Journal of Taxonomy 322, 1–44.
Lin, C.-H., Chang, C.-W., 2012. Otolith atlas of Taiwan fishes. National Museum of Marine Biology and Aquarium, Pingtung.
Lin, C.-H., Girone, A., Nolf, D., 2015. Tortonian fish otoliths from turbiditic deposits in northern Italy: taxonomic and stratigraphic significance. Geobios 48, 249–261.
Lin, C.-H., Girone, A., Nolf, D., 2016. Fish otolith assemblages from Recent NE Atlantic sea bottoms: a comparative study of palaeoecology. Palaeogeography, Palaeoclimatology, Palaeoecology 446, 98–107.
Lin, C.-H., Taviani, M., Angeletti, L., Girone, A., Nolf, D., 2017b. Fish otoliths in superficial sediments of the Mediterranean Sea. Palaeogeography, Palaeoclimatology, Palaeoecology 471, 134–143.
Menezes, G.M., Sigler, M.F., Silva, H.M., Pinho, M.R., 2006. Structure and zonation of demersal fish assemblages off the Azores Archipelago (mid-Atlantic). Marine Ecology Progress Series 324, 241–260.
Mytilineou, C., Politou, C.-Y., Papaconstantinou, C., Kavadas, S., D'Onghia, G., Sion, L., 2005. Deep-water fish fauna in the Eastern Ionian Sea. Belgian Journal of Zoology 135, 229–233.
Nelson, J.S., Grande, T.C., Wilson, M.V.H., 2016. Fishes of the world, Fifth Edition. John Wiley & Sons, Hoboken, New Jersey.
Nicolas, D., Lobry, J., Le Pape, O., Boet, P., 2010. Functional diversity in European estuaries: relating the composition of fish assemblages to the abiotic environment. Estuarine, Coastal and Shelf Science 88, 329–338.
Nolf, D., 1985. Otolithi Piscium. In: Schultze, H.P. (Ed.), Handbook of Paleoichthyology, 10. Fischer, Stuttgart, New York.
Nolf, D., 2013. The Diversity of Fish Otoliths, Past and Present. Royal Belgian Institute of Natural Sciences, Brussels.
Nolf, D., Brzobohatý, R., 1994. Fish otoliths from the Late Oligocene (Eger and Kiscell Formations) in the Eger area (northeastern Hungary). Bulletin de l'Institut royal des Sciences naturelles de Belgique, Sciences de la Terre 64, 225–252.
Nolf, D., Brzobohatý, R., 2002. Otolithes de poissons du Paléocanyon de Saubrigues (Chattien à Langhien), Aquitaine méridionale France. Revue de Micropaléontologie 45, 261–296.
Nolf, D., Brzobohatý, R., 2004. Otolithes de poissons du Miocène inférieur piémontais. Rivista Piemontese di Storia Naturale 25, 68–118.
Nolf, D., Girone, A., 2006. Otolithes de poissons du Pliocène inférieur (Zancléen) des environs d'Alba (Piémont) et de la côte ligure. Rivista Piemontese di Storia Naturale 27, 77–114.
Oksanen, J., Blanchet, F.G., Kindt, R., Legendre, P., Minchin, P.R., O'Hara, R.B., Simpson, G.L., Solymos, P., Stevens, M.H.H., Wagner, H., 2013. Package 'vegan'. , In: http://cran.r-project.org/web/packages/vegan/index.html.
Ormond, R.F.G., Edwards, A., 1987. Red Sea Fishes. In: Edwards, A.J., Head, S.M. (Eds.), Red Sea. Pergamon Press, Oxford, pp. 252–287.
Parin, N.V., Kobyliansky, S.G., 1993. Review of the genus *Maurolicus* (Sternoptychidae, Stomiiformes), with reestablishing validity of five species considered junior synonyms of *M. muelleri* and descriptions of nine new species. Trudy Okeanologii Instituta, Akademia Nauk, USSR 128, 69–107.
Patarnello, T., Volckaert, F., Castilho, R., 2007. Pillars of Hercules: is the Atlantic-Mediterranean transition a phylogeographical break? Molecular Ecology 16, 4426–4444.
Přikryl, T., Brzobohatý, R., Gregorová, R., 2016. Diversity and distribution of fossil codlets (Teleostei, Gadiformes Bregmacerotidae): review and commentary. Palaeobiodiversity and Palaeoenvironments 96, 13–39.
Pusch, C., Beckmann, A., Porteiro, M., von Westernhagen, H., 2004. The influence of seamounts on mesopelagic fish communities. Archives of Fishery and Marine Research 51, 165–186.
Core Team, R., 2012. R: a language and environment for statistical computing. Vienna, Austria.
Righton, D., Kemp, J., Ormond, R., 1996. Biogeography, community structure and diversity of Red Sea and Western Indian Ocean Butterflyfishes. Journal of the Marine Biological Association of the United Kingdom 76, 223–228.

Rivaton, J., Bourret, P., 1999. Les otolithes des poissons de l'Indo-Pacifique. Documents scientifiques et techniques. Institut de Recherche pour le Développement, Nouméa 2 (2), 1–378.
Sartori, R., 1977. I campioni prelevati dal Laboratorio di Geologia Marina negli anni 1967-1974. Dati essenziali. Rapporto Tecnico. Consiglio Nazionale delle Ricerche, Laboratorio per la Geologia Marina, Bologna.
Schwarzhans, W., 2013a. Otoliths from dredges in the Gulf of Guinea and off the Azores – an actuo-paleontological case study. Palaeo Ichthyologica 13, 7–40.
Schwarzhans, W., 2013b. A comparative morphological study of the Recent otoliths of the genera *Diaphus Idiolychnus and Lobianchia* (Myctophidae). Palaeo Ichthyologica 13, 41–82.
Smale, M.J., Watson, G., Hecht, T., 1995. Otolith Atlas of Southern African Marine Fishes Ichthyological Monographs of the J.L.B. Smith Institute of Ichthyology 1, 1–253.
Tuset, V.M., Lombarte, A., Assis, C.A., 2008. Otolith atlas for the western Mediterranean, north and central Eastern Atlantic. Scientia Marina 72S1 1–203.
Whitehead, P.J.P., Bauchot, M.L., Hureau, J.C., Nielsen, J., Tortonese, E. (Eds.), 1986. Fishes of the North-eastern Atlantic and the Mediterranean.. UNESCO, Paris, vol. 1 (1989), 1-510, vol. II (1986), 511-1007, vol. III, pp. 1008-1473. (1986-1989).
Wigley, R.L., Stinton, F.C., 1973. Distribution of macroscopic remains of Recent animals from marine sediments off Massachusetts. Fishery Bulletin 71, 1–40.